

Package *FLUIDS*. Part 4: thermodynamic modelling and purely empirical equations for H₂O-NaCl-KCl solutions

Ronald J. Bakker

Received: 16 July 2011 / Accepted: 10 January 2012
© Springer-Verlag 2012

Abstract A H₂O-NaCl-KCl-rich fluid occurs occasionally in fluid inclusions in a variety of geological environments. The properties of this fluid provide information about the conditions of entrapment, and thereby, conditions that have affected the rock. New purely empirical and thermodynamic models are developed in this study to reproduce the properties of the H₂O-NaCl-KCl fluid system, especially the *liquidus* at variable pressures (the solid–liquid–vapour surface, i.e. *SLV*), and at constant pressures (the solid–liquid surface, i.e. *SL*). The *SLV* surface is modelled according to “best-fit” polynomial equations, which relate temperature, pressure and composition. The *SL* surfaces, at constant pressures, are modelled according to thermodynamic principles, i.e. the equality of chemical potentials of components (NaCl and KCl) in each phase at equilibrium. The models are valid up to 400 MPa and 900°C and can be applied to fluid inclusions studies to obtain salinities from dissolution temperatures of salt crystals. The new models are included in the program *AqSo WHS* that forms part of the software package *FLUIDS* (Bakker, Chem Geol 194:3–23, 2003), to be able to apply directly the mathematical functions in fluid inclusion studies and in general fluid properties investigations.

Introduction

H₂O-salt fluid mixtures are common phases in a variety of geological environments and are involved in many processes, e.g. in evaporitic basins (e.g. Sabouraud 1994), diagenesis of sediments (e.g. Goldstein and Reynolds 1994), ore mineralization (e.g. Wilkinson 2003), and magmatic processes (e.g. Kamenetsky et al. 2006). NaCl is one of most common salt types that are found in fluid inclusions, and the binary H₂O-NaCl system (Fig. 1a) can be thermodynamically modelled by relatively simple mathematical means. Traditionally, only parts of the pressure (*p*)–temperature (*T*)–volume (*V*)–amount of substance (*n*) parameter space of this fluid system were modelled. The amount of substance fraction is also known as “mole” fraction (*x*) (see Taylor 1995). The H₂O-NaCl system was described by purely empirical sub-parameters, i.e. a parameter that is indirectly related to physical properties of the water-salt system. For example, the freezing point depression of ice have been described by simple polynomial fits of the second grade up to 23 mass% NaCl (e.g. Potter et al. 1978; Hall et al. 1988; Bodnar 1993). In addition, higher-grade polynomial fits have been used to calculate the salinity from halite dissolution temperatures (e.g. Sterner et al. 1988; Driesner and Heinrich 2007). KCl is a second common salt type that may regularly occur in geological fluids (e.g. Campbell et al. 2001). The fluid properties of a KCl-rich aqueous solution in fluid inclusion studies have only been described as part of the ternary H₂O-NaCl-KCl fluid system (e.g. Sterner et al. 1988; Bodnar et al. 1989).

The *liquidus* of the ternary H₂O-NaCl-KCl system has been thermodynamically determined by modelling activity coefficients of NaCl and KCl (Chou 1982; Gunter et al. 1983; Chou 1987; Chou et al. 1992; Sterner et al. 1992). This

Editorial handling: J. G. Raith

Electronic supplementary material The online version of this article (doi:10.1007/s00710-012-0192-z) contains supplementary material, which is available to authorized users.

R. J. Bakker (✉)
Department of Applied Geosciences and Geophysics,
University of Leoben,
Peter-Tunner-Str. 5,
8700 Leoben, Austria
e-mail: bakker@unileoben.ac.at

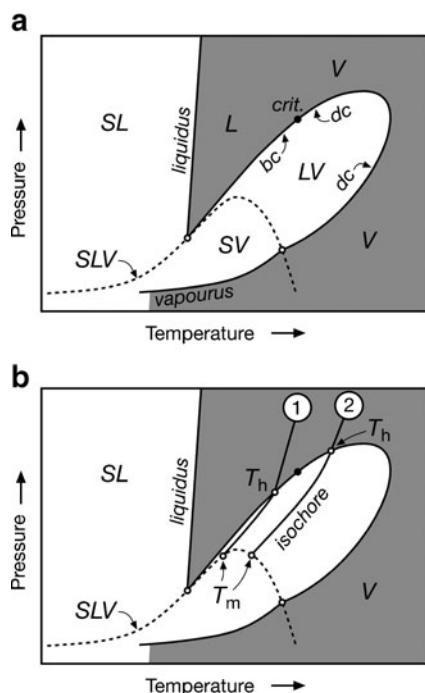


Fig. 1 **a** Isoleth in a schematic temperature-pressure diagram in a binary water-salt fluid system. The *liquidus*, bubble point curve (*bc*), critical point (*crit.*), dew point curve (*dc*), and vapourus separate a homogeneous fluid field from two-phase fields (*LV*, *SV*, and *SL*) and a three-phase line (*SLV*). The homogeneous fluid can be liquid-like (*L*) or vapour-like (*V*), which can be deduced from the mode of homogenisation of fluid inclusions. Note that the critical point is not located at maximum temperature or maximum pressure of the *LV*-envelope. The *liquidus* is being modelled in this study and is nearly vertical. *S* = solid halite crystal, *L* = brine, *V* = vapour. **b** Schematic isochores (1. liquid-like fluid; 2. vapour-like fluid) in the same temperature-pressure diagram, indicating the relationship between total homogenisation temperatures (T_h) and dissolution temperatures (T_m) of salt crystals, that are not located at the *liquidus* curve. The inclusion with isochore 1 homogenises in the liquid phase, and the inclusion with isochore 2 in the vapour phase

model was not applied to fluid inclusions studies, although the melting of a salt crystal in a brine in the absence of a vapour phase at higher temperatures is a common phenomenon that can be often observed in fluid inclusions. The best-fit equations that were obtained for the interaction parameters between H_2O , $NaCl$, and KCl molecules (Stern et al. 1992) are only poorly reproducing values that are calculated from experimental data. Moreover, these equations cannot be extrapolated below $450^\circ C$ and 50 MPa, and above 200 MPa this model is defined by only three experimental data points from Gunter et al. (1983). Therefore, this equation cannot be used to calculate the *SLV* surface (e.g. Fig. 1) that is generally used in fluid inclusion studies.

In theory according to the Gibbs phase rule, dissolution temperatures of salt crystals cannot be used directly to calculate bulk salinities of fluid inclusions (Bakker 2012). Bulk

salinities and densities in binary water-salt systems can only be obtained by combining dissolution temperatures (e.g. $SLV \rightarrow LV$) and total homogenisation temperatures (e.g. $LV \rightarrow L$). The dissolution temperature is highly dependent on the bulk density of the fluid inclusion (Fig. 1b). An assemblage of inclusions with the same bulk salinity and variable density display highly variable dissolution temperatures of salt crystals. This phenomenon was identified by Stern et al. (1988), but it was assumed to have a negligible effect on the melting temperatures and it was not further investigated. The extent of erroneously determined salinities from only melting temperatures can be illustrated with an example: a fluid inclusion with a bulk composition of 40 mass% $NaCl$ and 60 mass% H_2O , and a bulk molar volume of $28.48 \text{ cm}^3 \cdot \text{mol}^{-1}$ has a total homogenisation into the liquid phase at $600^\circ C$ and 79.5 MPa (calculated with computer package “*FLUIDS*” program *LonerAP*, Bakker 2003, using the equation of state of Anderko and Pitzer 1993). The isochore of this fluid intersects the *SLV* curve at $367.2^\circ C$, where a salt cube crystallizes during cooling. At this temperature, the inclusion contains a nearly pure H_2O vapour phase (volume fraction of vapour: $\varphi^{vap}=0.181$) and a saturated brine (40.5 mass% $NaCl$). According to Bodnar et al. (1989), a fluid inclusion with 40 mass% $NaCl$ has a halite dissolution temperature of $326^\circ C$ in the presence of a vapour. At $367.2^\circ C$ they predict a bulk salinity of 44 mass% $NaCl$.

The *liquidus* of the ternary system H_2O - $NaCl$ - KCl , i.e. the phase boundary where a crystal of either ice, hydrohalite, halite or sylvite (as schematically illustrated for a water-salt system in Fig. 1a) is completely dissolved in a liquid aqueous solution, in the absence and presence of a vapour bubble within fluid inclusions, is re-examined in this study because previous research has illustrated inconsistencies between thermodynamic modelling according to equilibrium criteria and purely empirical fittings (c.f. Stern et al. 1988; Stern et al. 1992). Furthermore, the published polynomial equations are, in part, not reproducible and inconsistent in compositional phase diagrams. The present study provides a new set of empirical polynomial best-fit equations that relate dissolution temperatures and pressures of hydrohalite (i.e. hydrohalite field), halite (i.e. halite field), and sylvite (i.e. sylvite field) with compositions in the ternary H_2O - $NaCl$ - KCl fluid system. In addition, the activity coefficients of $NaCl$ and KCl are modelled according to equilibrium thermodynamics, and new definitions for the interaction parameters are developed in this study, in order to reproduce accurately experimental data. The new equations can also be used for the three subordinate binary systems, i.e. H_2O - $NaCl$, H_2O - KCl and $NaCl$ - KCl systems. These new equations are included in the software package *FLUIDS* (Bakker 2003), in the program *AqSo WHS*, that has been designed to model the salinity of fluid inclusions according to dissolution temperatures (see Appendix A).

Experimental data

Linke (1965) presented the solubility and density data of NaCl, KCl and mixtures of NaCl-KCl in H₂O in the liquid phase available at that time. Summarized, the binary NaCl-H₂O system has an eutectic point at -21.2°C and 23.3 mass% NaCl in the presence of ice and hydrohalite. The peritectic point is at +0.1°C and 26.3 mass% NaCl, where hydrohalite reacts to halite. The eutectic point of the binary H₂O-KCl is at -10.6°C and 19.7 mass% KCl. In the ternary system, the eutectic and peritectic point are defined at -22.9°C (5.81 mass% KCl and 20.17 mass% NaCl) and -2.3°C (6.98 mass% KCl and 22.54 mass% NaCl), respectively.

The *liquidus* of the binary anhydrous NaCl-KCl system was studied by Chou (1982) and Pelton et al. (1985) using a differential thermal analytical technique (*DTA*). Bukhalova and Bergman (1955) and Rubleva and Bergman (1956) analysed this *liquidus* as part of quaternary and ternary salt solutions, respectively. The *solidus* of the binary anhydrous NaCl-KCl system was estimated by Heide and Brückner (1967), Luova and Muurien (1967) and Chou et al. (1992). At 0.1 MPa, *solidus* and *liquidus* coincide at a minimum temperature of about 658°C and about 43.9 mass% NaCl. At lower temperatures, the anhydrous NaCl-KCl system has a *solvus* below approximately 490°C, where the solid solution separates in NaCl-rich crystals and KCl-rich crystals (Bunk and Tichelaar 1953; Barrett and Wallace 1954; Chanh 1964; Vesnin and Zakovryashin 1979).

The vapour pressure of binary NaCl-H₂O and KCl-H₂O systems (*SLV* line in Fig. 1) was estimated by Keevil (1942), Sourirajan and Kennedy (1962), and Chou (1987). Ravich and Borovaya (1949, 1950) provided data on the vapour pressure of saturated solutions in the ternary H₂O-NaCl-KCl system. At higher pressures, the *liquidus* of this ternary system was determined by Chou et al. (1992, and reference therein).

Hall et al. (1988) provided data on the *liquidus* in the ternary H₂O-NaCl-KCl system by gravimetric analysis at various temperatures and room pressure for an aqueous solution in equilibrium with ice (i.e. the ice field). It is assumed that these data can be applied to the final melting temperature of ice in fluid inclusions. Hall et al. (1988) provided a polynomial best fit of the third degree to reproduce their data. It can be applied in the entire ice field of this system. The data from Linke (1965) were not included in these fitting procedures.

Synthetic fluid inclusion studies were also used to determine salinities from melting temperatures in the ternary H₂O-NaCl-KCl system. For example, Hall et al. (1988) reproduced the eutectic point in terms of composition and temperature in the binary H₂O-NaCl in synthetic fluid inclusions. Synthetic fluid inclusions were also used to obtain data in the halite and sylvite field (Sterner et al. 1988). Polynomial fits up to the ninth degree were provided, to calculate salinities from the final melting of halite and sylvite in the ternary system in the

presence of a vapour phase. Data for the hydrohalite field were not obtained in synthetic fluid inclusion studies, and it was only represented by a first-degree polynomial fit in the triangular compositional diagram of the H₂O-NaCl-KCl system.

Fluid inclusions may also reveal a different homogenization behaviour upon heating, i.e. first the vapour phase disappears (*SLV*→*SL*), followed by a total homogenization by dissolution of a salt crystal in the liquid phase (*SL*→*L*) (e.g. Bodnar 1994 for a 40 mass% NaCl solution). For a variety of salinities, Becker et al. (2008) has provided experimental data that relate these temperatures with the pressure in fluid inclusions (up to 300 MPa). Unfortunately, the exact salinities of these fluid inclusions are unknown, but were calculated by using the *SLV*-curve defined by Bodnar (1992, abstract only), and the slope of the *liquidus* in *p-T* space (Bodnar 1994). These definitions of the *liquidus* are inconsistent with the experimental data from Chou et al. (1992) and the thermodynamically modelled *liquidus* according to Sterner et al. (1992).

The earlier purely empirical models based on fluid inclusion research

Isotherms

Polynomial fits up to the ninth degree of the halite field, sylvite field (Sterner et al. 1988), and the ice field (Hall et al. 1988) in the ternary H₂O-NaCl-KCl system are used in the computer program *SALTY* (Bodnar et al. 1989) to calculate salinities from melting (i.e. dissolution) temperatures. Bakker (2003) developed the program *AqSol* in the package *FLUIDS* using the same equations to obtain similar results with C++ and a SIOUX interface that runs on both Windows and Macintosh operated computer systems. These programs can be used to recalculate isotherms in compositional diagrams (i.e. lines of equal dissolution temperatures of either ice, halite or sylvite) as given in Fig. 3 from Sterner et al. (1988), and can also be used to compare experimental data, that include total salinity (i.e. the sum of NaCl and KCl) and corresponding final dissolution temperatures with calculated isotherms. The reproduced isotherms illustrated in Fig. 2 are substantially different from those presented by Sterner et al. (1988). Above 500°C, isotherms contain a number of inflection points that cannot be justified by the amount of available data. The lack of data does not allow polynomial fitting at higher degrees, but inevitably results in “*over-fitting*” when it is applied, as evidenced by numerous inflection points. The experimental data in the ternary H₂O-NaCl-KCl are mainly distributed at higher H₂O mole fractions (Fig. 2). Second, isotherms that are calculated with the equations designed for the halite field and the adjacent sylvite field at the same temperature do not intersect at the minimum (i.e. approximate

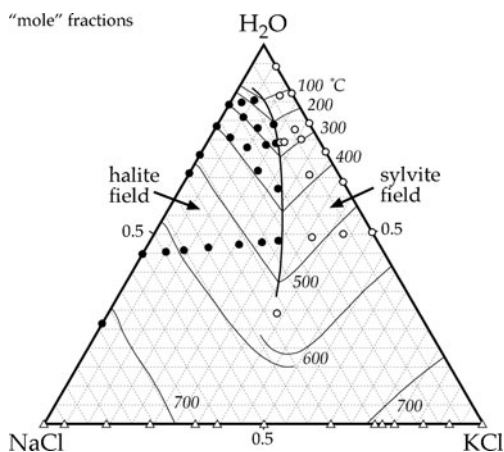


Fig. 2 Vapour saturated *liquidus* in a compositional diagram (in “mole” fractions) of the H₂O-NaCl-KCl system at variable pressures (not indicated) according to Sterner et al. (1988). The curved thin lines are isotherms at 100, 200, 300, 400, 500, 600, and 700°C. The thick curve is the cotectic line between the halite and the sylvite fields. The experimental data from Sterner et al. (1988) are illustrated with black dots (halite field) and open circles (sylvite field). The open triangles are data of the *liquidus* in the binary NaCl-KCl sub-system from Chou (1982)

extension of the cotectic line) above 500°C (e.g. see the 600°C isotherms in Fig. 2).

Total salinity in fluid inclusions containing a NaCl and KCl crystal is obtained from the final dissolution temperature of the first salt component that occurs at the cotectic line in the presence of the other salt component, and the final dissolution temperature of the second salt component, that is reflected by the isotherms within a specific field. The deviation of experimentally determined vapour-saturated solubilities and calculated values in the halite and sylvite field is highly underestimated by Sterner et al. (1988). Their uncertainty-analyses are based on the sum of NaCl and KCl contents in the inclusions and do not reveal the deviation of individual compounds. Several recalculated deviations of individual NaCl and KCl contents are given in Table 1, and illustrate relative large differences between calculated and experimental data. All experimental data illustrate opposite deviation trends for NaCl and KCl couples. A large positive deviation in KCl contents and a large negative deviation in NaCl contents always result in an accurate but meaningless approach of the total salinity. For example, an experimental total salinity of 80.0 mass% consists of 70.84 mass% NaCl and 9.16 mass% KCl (see Table 1). The calculations according to Sterner et al. (1988) by using the dissolution temperatures result in a total salinity of 82.23 mass%, that consists of 66.68 mass% NaCl and 15.55 mass% KCl. The total salinity deviates only about 2.23 mass%, whereas the calculated NaCl content is about 6% lower and the KCl content is about 70% higher than the experimental values. In other words, a complete uncertainty analysis must also include the NaCl-KCl mass ratio comparison.

Table 1 Comparison between experimental data from Sterner et al. (1988) and calculated salinities using the equations given in Sterner et al. (1988). The uncertainty in calculated values is obtained from the range in experimental data and by taken into account the accuracy in temperature measurements, i.e. ± 2.5°C above 50°C, ± 3°C between 375 and 575°C

Total salinity (mass%)	Type of salt	Experimental mass%	Calculated mass%	Difference
37.8	NaCl	22.24	21.61±0.35	-0.63
	KCl	15.56	16.74±0.48	+1.18
45.0	NaCl	31.10	29.55±0.50	-1.55
	KCl	13.90	17.69±0.50	+3.79
52.4	NaCl	40.48	37.99±0.93	-2.49
	KCl	11.92	17.43±0.50	+5.51
57.0	NaCl	16.95	17.68±0.12	+0.73
	KCl	40.05	39.78±0.51	-0.27
64.5	NaCl	30.79	30.06±0.67	-0.73
	KCl	33.71	36.52±0.53	+2.81
80.0	NaCl	18.90	21.17±0.72	+2.27
	KCl	61.10	59.74±1.06	-1.36
80.0	NaCl	70.84	66.68±2.06	-4.16
	KCl	9.16	15.55±0.55	+6.39

Cotectic lines

The cotectic lines in the ternary H₂O-NaCl-KCl compositional diagram are defined by the intersection of isotherms of adjacent fields (e.g. halite- and sylvite field). To facilitate the mathematical calculations, these intersection points were fitted to additional polynomial functions (see Bodnar et al. 1989) that, however, reduce the accuracy of salinity calculations (Fig. 3). The use of this additional fit at the cotectic line is adding an extra deviation up to 2% at relative low temperatures (below 100°C). The individual deviations of

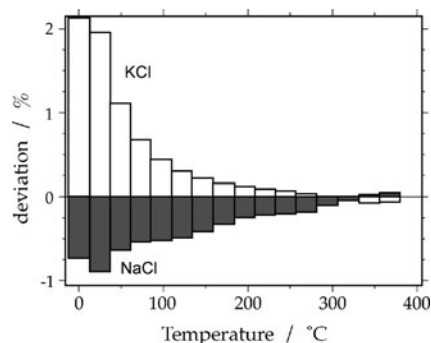


Fig. 3 Comparison between calculated salinity of individual NaCl and KCl content (in mass%) along the cotectic line according to the equations from Bodnar et al. (1989) and values obtained from the exact isotherm intersection between the adjacent halite- and sylvite-field. The deviation is defined as the difference in mass fractions between Bodnar’s model and the exact intersection, divided by the mass fraction according to Bodnar et al. (1989), in percentage

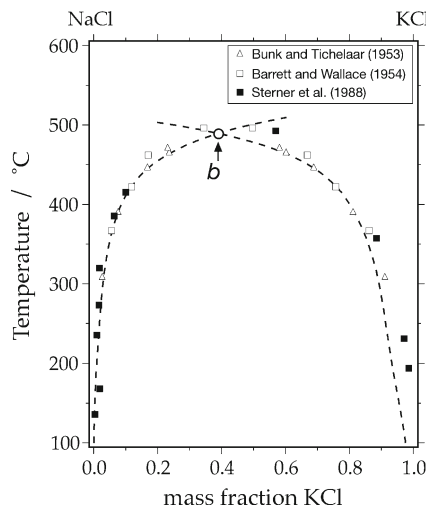


Fig. 4 Solvus in the anhydrous NaCl-KCl system. Experimental data are compared with best-fit equations according to Bodnar et al. (1989), see dashed lines. The open circle (b) illustrates the fixed maximum of the solvus, that was defined by Bunk and Tichelaar (1953)

the NaCl and KCl salinity also display an opposite trend, and increase towards lower temperatures.

Solvus in the binary NaCl-KCl sub-system

Polynomial best-fit equations of the eighth degree were defined in the computer program “SALTY” (Bodnar et al. 1989) to reproduce experimental data of the solvus in the binary NaCl-KCl system. The solvus equation was split in two parts (Fig. 4) due to the difficulty to fit the shape of the entire solvus to one polynomial function, in which temperature is described as a function of mass fraction. These two parts intersect by definition at 490°C and 61 mass% NaCl. Consequently, the solvus displays a discontinuous curve at the intersection point. Re-examination of these equations illustrates a poor fit to the available data (see Fig. 4), and thermodynamically modelled solvi according to Waldbaum (1969) and Green (1970).

New polynomial fitting procedures for vapour saturated conditions

Liquidus

The experimental data of dissolution temperatures and composition in the halite-, sylvite-, and hydrohalite field from Linke (1965), Chou (1982), and Sterner et al. (1988) are used in this study to obtain new polynomial best-fit equations to describe the liquidus temperature of the ternary system H₂O-NaCl-KCl in the presence of a vapour phase at variable pressures (i.e. the SLV surface).

The polynomial fitting is performed in several steps within a triangular compositional diagram, either in “mole” fractions

or mass fractions. Firstly, interpolation of experimental data is based on non-linear polynomial fitting to at least three data points that align in the triangular diagram (e.g. line 1 and 2 in Fig. 5a). These best-fit equations are expressed in $x(H_2O)$ as a function of the relative amount of NaCl in the NaCl-KCl binary sub-system, i.e. R_{NaCl} (Eq. 1a, Fig. 5b), and final dissolution temperature (T_m) as a function of R_{KCl} , i.e. the relative amount of KCl, (Eq. 1b, Fig. 5c).

$$R_{NaCl} = \frac{x(NaCl)}{x(NaCl) + x(KCl)} \quad (1a)$$

$$R_{KCl} = \frac{x(KCl)}{x(NaCl) + x(KCl)} \quad (1b)$$

where x is “mole” fraction in the ternary system. Secondly, interpolated data at selected R_{NaCl} values are obtained from a series of these polynomial fits through a variety of data. For example line 1 in Fig. 5, at a relative NaCl fraction of 0.8 the temperature is 582.45°C and the $x(H_2O)$ is 0.4612. Various intersections with the $R_{NaCl}=0.8$ are collected from a variety of interpolations, and the corresponding pairs of T_m and $x(H_2O)$ are plotted in a new diagram (Fig. 6). Subsequently, these interpolated data are fitted to new polynomial functions that calculate the $x(H_2O)$ as a function of temperature for one specific R_{NaCl} value (Eq. 2).

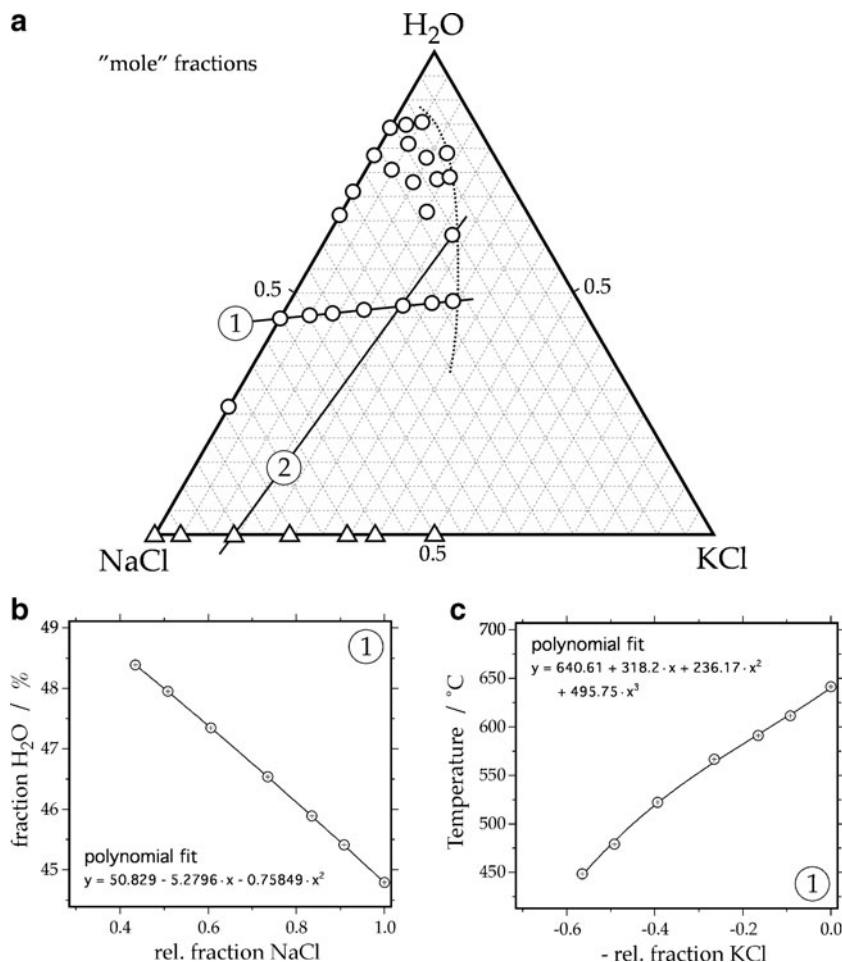
$$x(H_2O) = \sum_i k_i \cdot T^i \quad (2)$$

where $x(H_2O)$ is the mole fraction of H₂O in the ternary H₂O-NaCl-KCl system, T is the dissolution temperature (in °C) at the liquidus at variable pressures, k_i are constants for a specific R_{NaCl} , and i is an integer. This integer has a value of 2, 4 and 5 for the hydrohalite field, sylvite field and the halite field, respectively. The number of experimental data in the hydrohalite field is only few, therefore, polynomial fitting is limited to a lower degree.

For the halite field eight relative fractions of NaCl are selected: 1.0 (pure NaCl), 0.9, 0.8, 0.7, 0.6, 0.5, 0.435, and 0.4, and for the sylvite field nine relative fractions of NaCl are selected: 0.0 (pure KCl), 0.1, 0.2, 0.3, 0.4, 0.5, 0.6, 0.7, and 0.8 to perform the interpolation procedures. Finally, the values obtained for the “ k ” parameter in individual fields are modelled in a function of R_{NaCl} , or R_{KCl} , using new polynomial best-fit equations up to the seventh degree. The final polynomial equations that relate dissolution temperatures and composition in the ternary H₂O-NaCl-KCl system in the hydrohalite field, halite field and sylvite field are defined according to Eqs. 3(a, b), 4(a, b) and 5(a, b), respectively. The values of the parameters in these equations are given in Tables 2, 3, and 4, respectively.

$$x(H_2O)^{HH} = a_0 + a_1 \cdot T_C + a_2 \cdot T_C^2 \quad (3a)$$

Fig. 5 Compositional triangular diagram of the liquidus in the H₂O-NaCl-KCl system with experimental data and interpolation lines **a**. Open circles are data from Sterner et al. (1988), open triangles are data from Chou (1982). Best fit polynomial functions for line *l* are illustrated in **b** and **c**. See text for further details



$$a_i = \sum_j a_{ij} \cdot (R_{NaCl})^j \quad (3b)$$
 where, T_C is temperature in °C and R_{NaCl} is the relative fraction of NaCl (varying between 0.8 and 1.0). The integer j varies

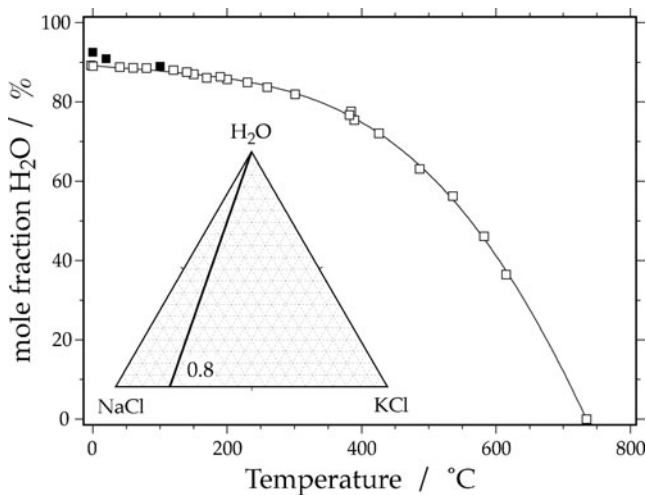


Fig. 6 Liquids in the ternary H₂O-NaCl-KCl system at a constant ratio of $R_{NaCl}=0.8$. The open squares are interpolated data obtained from various interpolation lines as illustrated in Fig. 5. Solid squares are rejected interpolated data. The new best-fit polynomial curve is defined according to Eq. 2

between 0 and 2. The superscript *HH* indicates the hydrohalite field.

$$x(H_2O)^H = b_0 + b_1 \cdot T_C + b_2 \cdot T_C^2 + b_3 \cdot T_C^3 + b_4 \cdot T_C^4 + b_5 \cdot T_C^5 \quad (4a)$$

$$b_i = \sum_j b_{ij} \cdot (R_{KCl})^j \quad (4b)$$

where, T_C is temperature in °C and R_{KCl} is the relative fraction of KCl (varying between 0.0 and 0.65). The superscript *H* indicates the halite-field. The integer j varies between 0 and 3. In addition, the variable b_0 also includes the parameters for $j=5$ ($b_{05}=122.8$), $j=6$ ($b_{06}=-732.39$) and $j=7$ ($b_{07}=742.95$).

$$x(H_2O)^S = c_0 + c_1 \cdot T_C + c_2 \cdot T_C^2 + c_3 \cdot T_C^3 + c_4 \cdot T_C^4 \quad (5a)$$

Table 2 Values of the a_{ij} parameters in Eq. 3 for the hydrohalite field

	$j=0$	$j=1$	$j=2$
a_0	84.289	5.8318	–
a_1	0.10814	-0.43499	0.27882
a_2	-0.011262	0.023776	-0.01173

Table 3 Values of the b_{ij} parameters in Eq. 4 for the halite field

	$j=0$	$j=1$	$j=2$	$j=3$
b_0	90.1206	-5.2839	-4.5899	24.3
b_1	-0.0023261	-0.035774	–	–
b_2	$-7.8436 \cdot 10^{-5}$	0.00028266	–	–
b_3	$2.1344 \cdot 10^{-7}$	$-8.4643 \cdot 10^{-7}$	$1.9831 \cdot 10^{-7}$	$-2.8168 \cdot 10^{-6}$
b_4	$-5.6929 \cdot 10^{-10}$	$7.6347 \cdot 10^{-10}$	$-6.6397 \cdot 10^{-10}$	$4.8428 \cdot 10^{-9}$
b_5	$2.627 \cdot 10^{-13}$	$-1.8389 \cdot 10^{-13}$	$-2.1647 \cdot 10^{-12}$	$2.7548 \cdot 10^{-12}$

$$c_i = \sum_j c_{ij} \cdot (R_{NaCl})^j \quad (5b)$$

where, T_C is temperature in °C and R_{NaCl} is the relative fraction of NaCl (varying between 0.0 and 0.81). The superscript S indicates the sylvite field. The integer j varies between 0 and 2. In addition, the variable c_4 also includes the parameters for $j=3$ ($c_{43}=1.9585 \cdot 10^{-9}$) and $j=4$ ($c_{44}=-8.5994 \cdot 10^{-11}$). The parameters c_0 and c_1 (i.e. $i=0$ and 1) are not included in Table 4 because they are better defined according to exponential functions (Eq. 6a and 6b, respectively).

$$c_0 = 94.678 - 7.46512 \cdot \exp(-1.95722 \cdot R_{KCl}) - 15.1276 \cdot \exp(-15.1442 \cdot R_{KCl}) \quad (6a)$$

$$c_1 = -0.0668981 - 0.107838 \cdot \exp(-6.98181 \cdot R_{KCl}) \quad (6b)$$

The Eqs. 4(a, b) and 5(a, b) have been used to construct isotherms in the halite- and sylvite field, respectively (Fig. 7). The calculated isotherms contain less inflection points as obtained from the equations from Sterner et al. (1988) (c.f. Fig. 1), and isotherms of adjacent fields intersect at the cotectic or minimum curve of the *liquidus* surface.

The pressure at the vapour saturated *liquidus* in the halite field and sylvite field in the ternary H₂O-NaCl-KCl system is defined according to Eq. 7

$$p = d + e \cdot R_{NaCl} + f \cdot R_{NaCl}^2 \quad (7)$$

where p is pressure (in MPa), R_{NaCl} is the relative fraction of NaCl (see Eq. 1a), and d , e , and f are parameters that depend on temperature according to polynomial equations

Table 4 Values of the c_{ij} parameters in Eq. 5 for the sylvite field

	$j=0$	$j=1$	$j=2$
c_2	0.000145926	$-2.178 \cdot 10^{-5}$	-0.00016211
c_3	$-3.5848 \cdot 10^{-7}$	$-3.5629 \cdot 10^{-7}$	–
c_4	$1.0423 \cdot 10^{-11}$	$3.3412 \cdot 10^{-10}$	$-4.3135 \cdot 10^{-10}$

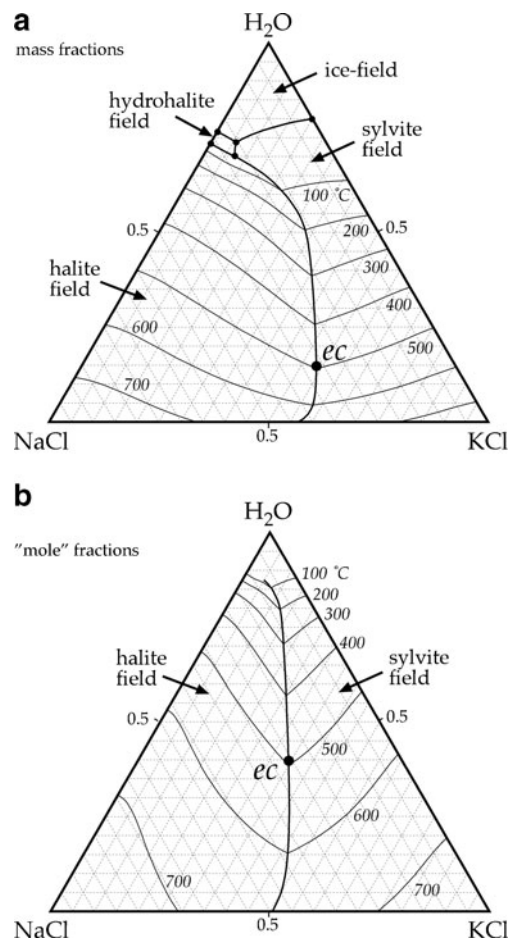


Fig. 7 Vapour saturated *liquidus* surface in the ternary H₂O-NaCl-KCl system in mass fractions **a** and “mole” fractions **b**. The four fields, i.e. ice-, hydrohalite-, halite-, and sylvite-field represent the stability of these solid phases with a brine and vapour. The fields are separated by cotectic curves. The thin solid lines are isotherms (in °C) of final dissolution of these solid phases in the brine. The solid phase at the maximum temperature of the *solvus* (495.1°C) in the anhydrous binary NaCl-KCl system is in equilibrium with a brine at point (*ec*), which correspond to the end-point of the cotectic curve between the halite- and sylvite field. At higher temperatures, the minimum is defined by the intersection of both fields. This type of purely empirical fitting does not allow a distinction between cotectic and minimum

(Eqs. 8a, 8b). Equations 7 and 8(a, b) are valid between 200 and 650°C.

$$d = \sum_i d_i \cdot Q^i \quad (8a)$$

$$Q = (T_C - T_0)/800 \quad (8b)$$

where T_C is temperature (in °C), T_0 is 200°C, Q is an arbitrarily defined parameter to express temperature, and i is an integer that has a value between 0 and 6 in the halite field, and between 0 and 7 in the sylvite field. A similar equation is used for the parameter e and f . The values for d_i , e_i and f_i are given in Tables 5 and 6. Below 200°C, it is assumed that the pressure approaches 0.1 MPa. Due to the

Table 5 Halite field: coefficients for the d , e and f parameter in Eq. 8

i	d_i	e_i	f_i
0	0.75256	0.52636	-0.12016
1	15.562	14.081	-13.202
2	128.58	-442.05	446.98
3	-2240.0	10489.0	-7727.1
4	4684.6	-31176.0	25875.0
5	4948.3	10569.0	-17444.0
6	-12269.0	22891.0	-8696.2

lack of experimental data above 650°C, the pressure and composition at the vapour saturated *liquidus* are obtained from different equations (Eqs. 9a, 9b for the halite-field, Eq. 10a, 10b for the sylvite field)

$$x(H_2O)^H = g_0 + g_1 \cdot x(KCl) \tag{9a}$$

$$g_i = \sum_j g_{ij} \cdot p^j \tag{9b}$$

where x is the mole fraction of water (H_2O) and sylvite (KCl), p is the pressure (in MPa), and j is an integer that varies between 1 and 3. The superscript H indicates the halite field.

$$x(H_2O)^S = h_0 + h_1 \cdot x(NaCl) \tag{10a}$$

$$h_i = \sum_j h_{ij} \cdot p^j \tag{10b}$$

where x is the mole fraction of water (H_2O) and halite ($NaCl$), p is the pressure (in MPa), and j is an integer that varies between 1 and 4. The superscript S indicates the sylvite field. The values of the coefficients for the parameters g_i and h_i are given in Tables 7 and 8, respectively. Figure 8 illustrates isobars (in MPa) at the vapour saturated *liquidus* in the ternary H_2O - $NaCl$ - KCl compositional diagram. The distribution of experimental data (Fig. 8a) indicates that there is a relative large uncertainty in several parts of this diagram, e.g. in the halite

Table 6 Sylvite field: coefficients for the d , e and f parameter in Eq. 8

i	d_i	e_i	f_i
0	1.0394	-0.16783	-0.35811
1	18.206	20.501	-8.3786
2	61.329	-420.56	-76.987
3	574.41	2956.7	1103.9
4	-1713.2	-9690.3	-20596.0
5	1006.8	9066.6	98723.0
6	–	–	-162440.0
7	–	–	85207.0

Table 7 Coefficients for the parameter g in Eq. 9 for the halite field

	$j=1$	$j=2$	$j=3$
g_0	0.0096226	$-3.9359 \cdot 10^{-6}$	$1.7538 \cdot 10^{-6}$
g_1	0.020061	0.0017448	

field. The cotectic line (also known as *eutonic* solutions, see Ravich and Borovaya 1949) reveals a minimum pressure in the ternary system at any selected $x(H_2O)$. Maximum pressures are obtained in the binary H_2O - $NaCl$ system at 39.4 MPa (595°C, 73.3 mass% $NaCl$), and in the binary H_2O - KCl system at 22.3 MPa (565°C, 81.9 mass% KCl). The cotectic reveals a maximum pressure of 12.9 MPa at 546.4°C and a composition of $x(NaCl)=0.3139$ and $x(KCl)=0.4031$.

NaCl-KCl solvus

The entire experimental data set of the *solvus* in the binary $NaCl$ - KCl system cannot be fitted with a simple polynomial equation that relates exsolution temperatures and compositions. In order to describe accurately the *solvus*, a new fitting procedure is applied in this study. First, the experimental data above 400°C was fitted to a polynomial function of the fourth degree that calculates temperature as a function of mass fraction KCl between 0.08 and 0.81 (Eq. 11). The resulting extremum is defined by a maximum of 495.1°C at 59 mass% $NaCl$, i.e. $x(NaCl)=0.65$, which is consistent with the estimations from Barrett and Wallace (1954) and Waldbaum (1969), and significantly different from the values selected by Sterner et al. (1988).

$$T = 321.81 + 1141.3 \cdot w_{KCl} - 2733.1 \cdot w_{KCl}^2 + 3031.4 \cdot w_{KCl}^3 - 1562.2 \cdot w_{KCl}^4 \tag{11}$$

where T is temperature in °C, and w_{KCl} is the mass fractions of KCl in the KCl - $NaCl$ binary system.

Second, the experimental data of $NaCl$ -rich and KCl -rich solutions below 400°C were fitted to polynomial function of the fourth degree and the third degree, respectively (Eqs. 12a and 12b). These equations calculate the mass fraction as a function of temperature, between 0 and 400°C.

$$w_{NaCl} = 6.4438 \cdot 10^{-7} \cdot T^2 - 4.6914 \cdot 10^{-9} \cdot T^3 + 1.0923 \cdot 10^{-11} \cdot T^4 \tag{12a}$$

Table 8 Coefficients for the parameter h in Eq. 10 for the sylvite field

	$j=1$	$j=2$	$j=3$	$j=4$
h_0	0.030798	-0.0025605	0.00015204	$-2.8959 \cdot 10^{-6}$
h_1	-0.0085533	0.00036598	0.0003538	$-1.1178 \cdot 10^{-5}$

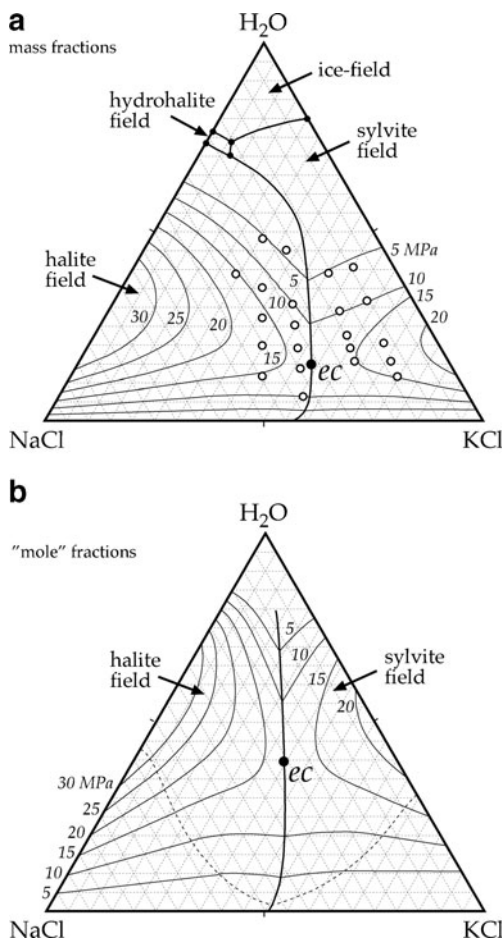


Fig. 8 Similar phase diagram as illustrated in Fig. 7 with isobars (in MPa). The open circles in **a** indicate the composition of experimental data from Ravich and Borovaya (1949). Experimental data from binary sub-systems, i.e. H₂O-NaCl and H₂O-KCl, are also used in the fitting procedures. The dashed line in **b** illustrates the 650°C isochore that defines the compositional boundary between Eqs. 7 and 9 in the halite field, and between Eqs. 7 and 10 in the sylvite field

$$w_{KCl} = 1 - 6.1237 \cdot 10^{-5} \cdot T + 9.9572 \cdot 10^{-7} \cdot T^2 - 5.1924 \cdot 10^{-9} \cdot T^3 \quad (12b)$$

where T is temperature in °C, w_{NaCl} and w_{KCl} are the mass fractions of NaCl and KCl, respectively, in the binary NaCl-KCl system. The Eqs. 11, 12a and 12b are designed to be continuous functions at the transition temperature 400°C.

Intersection of liquidus, solvus and solidus

Several pseudo-binary phase diagrams at constant H₂O composition are constructed from the ternary H₂O-NaCl-KCl compositional diagram (Fig. 9). The solid solution of NaCl and KCl is anhydrous at any temperature, pressure and bulk composition in this system. The NaCl-KCl system is characterised by an exsolution area defined by the *solvus* (*sv* in Fig. 9, calculated with Eqs. 11, 12a and 12b). NaCl and KCl mix completely in a single solid phase at temperatures above the *solvus*.

At 20 mass% H₂O (Fig. 9a), the anhydrous *solvus* intersects with the *solidus* and *liquidus* of the ternary system, which results in the formation of an eutectic point in the pseudo-binary system that corresponds to a cotectic point in the ternary system (point *c* in Fig. 9a). The *solidus* is only drawn schematically (dashed line in Fig. 9) because it is not defined by the previously described purely empirical fitting procedures. The cotectic point is richer in KCl mass fraction than the maximum of the *solvus* of the anhydrous salt phase. The pseudo-binary phase diagram (Fig. 9a) is a type V (Bakhuys-Roozeboom 1899) or type “e” (eutectic) according to Onck (1981). Within a small temperature interval between 15 and 17 mass% H₂O, the *solvus* intersects only the *solidus* and is positioned below the *liquidus* (Fig. 9b). As a consequence, a different type of phase diagram develops that contains

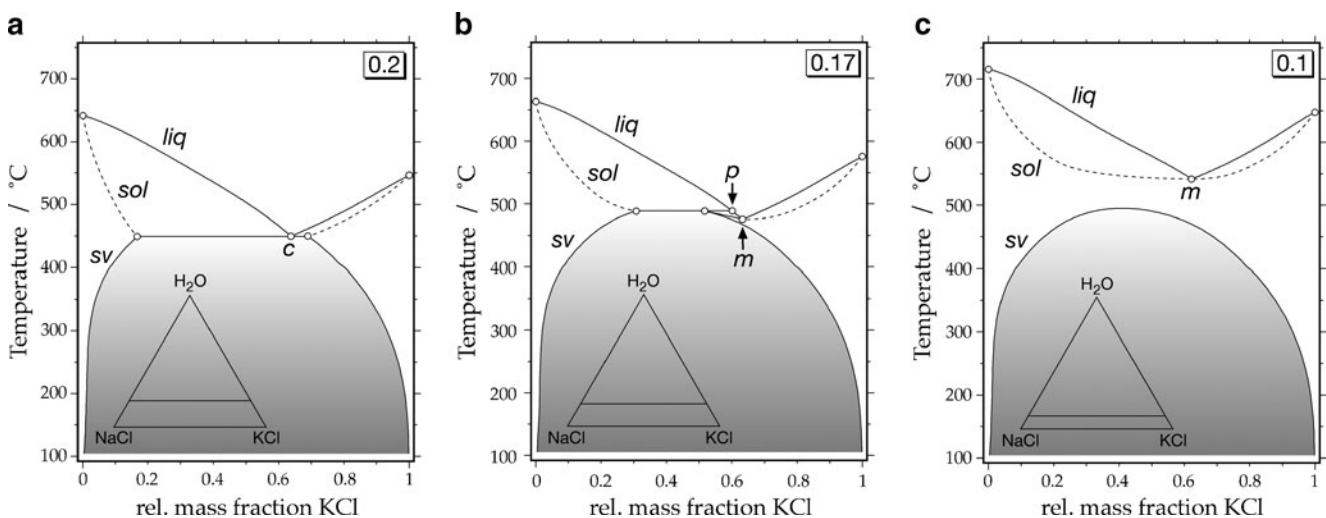


Fig. 9 Pseudo NaCl-KCl binary systems at 20 mass% H₂O **a**, 17 mass% H₂O **b** and 10 mass% H₂O **c**. See text for further details

a peritectic point in addition to a minimum, i.e. type “-*p*” according to Onk (1981). The minimum and peritectic are located closely. At 10 mass% H₂O (Fig. 9c), the *solvus* is completely separated from *liquidus* and *solidus*, which now reveal only a minimum at 542°C and 37.8 relative mass% NaCl (*m* in Fig. 9c). This phase diagram is of type III according to Bakhuis-Roozeboom (1899), or type “-” (minimum) according to Onk (1981). The properties of this transition cannot be obtained from purely empirical modelling that is presented in the previous paragraphs.

The pseudo-binaries in Fig. 9 are very unlike the consideration in Sterner et al. (1988) for the *SLV* curve in the ternary H₂O-NaCl-KCl system, but correspond to the calculated projections that were thermodynamically modelled at constant pressures (Sterner et al. 1992). In principle, the empirical models cannot be used to determine the salinities of fluid inclusions if the cotectic temperature exceeds 495.1°C, where the cotectic line is replaced by a minimum. By definition, the composition of the solid phase at higher temperatures is equal to the composition of the brine at the minimum (c.f. Fig. 11 in Sterner et al. 1988). However, the observation of one solid salt phase in fluid inclusions at higher temperatures does not imply that the system is located at the minimum curve.

Tielines at constant temperatures and pressures

Modelling the *SLV* surface (*liquidus*) with purely empirical best-fit equations does not allow the construction of tielines at selected constant temperatures and pressures, because the composition of the coexisting solid phase is unknown. However, at the cotectic line below the maximum temperature of the *solvus* (495°C) the exsolution of a homogeneous solid NaCl-KCl phase (see Eqs. 11, 12a and 12b) defines the composition of both a NaCl-richer salt crystal and a KCl-richer salt crystal, in the presence of a liquid and vapour phase. Figure 10 illustrates the development of the three-phase area with increasing temperature in the ternary compositional diagram.

The three-phase area (in the presence of the fourth phase: vapour) is defined by a liquid phase at the cotectic line (point *c* in Fig. 10a), a NaCl-rich solid salt phase (point *sol1* in Fig. 10a) and a KCl-rich solid salt phase (point *sol2* in Fig. 10a). The tielines within the two-phase field are schematically indicated, because the position of the intersection of tielines with the anhydrous NaCl-KCl base is unknown.

Close to the maximum *solvus* temperature (489°C in Fig. 10b), the three-phase area has become smaller, and is defined by a peritectic point (point *p* in Fig. 10b), that is positioned at slightly higher NaCl contents than the minimum at the *SLV* surface (point *m* in Fig. 10b). This situation corresponds to the pseudo-binary illustrated in Fig. 9b. The only tieline that is known in the two-phase field connects the minimum with an anhydrous homogeneous NaCl-KCl solid salt crystal of the same relative composition.

At higher temperatures (e.g. 600°C, Fig. 10c), the three-phase area does not exist, and the compositional triangular diagram displays only tielines between a completely miscible liquid phase, and a completely miscible solid phase. According to Sterner et al. (1988), the sketched tielines parallel to H₂O-NaCl base in the halite-field, and parallel to the H₂O-KCl base in the sylvite-field are substantial different from the considerations in this study.

Dissolution trajectories in fluid inclusion research

The composition of a brine in fluid inclusions that also contain a solid NaCl crystal, a solid KCl crystal and a vapour phase at room temperature is located on the cotectic curve within the ternary H₂O-NaCl-KCl diagram (see Fig. 7). During heating, both NaCl and KCl partly dissolve, whereas the composition of the brine moves along the cotectic curve. In addition, the solid NaCl crystal becomes enriched in KCl, and the KCl crystal becomes enriched in NaCl (*solvus*, see Fig. 9). The presence of unequal amounts of NaCl and KCl may result in complete dissolution of one of those salts at a certain

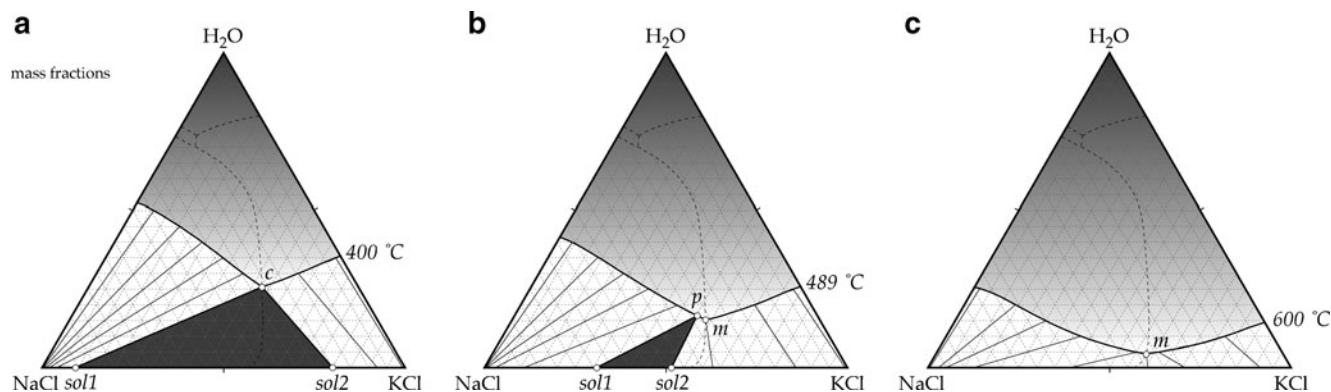


Fig. 10 Vapour saturated *liquidus* surface in the ternary H₂O-NaCl-KCl system in mass fractions at 400°C **a**, at 489°C **b**, and at 600°C **c**. *c* = cotectic point, *p* = peritectic point, *m* = minimum. The three-phase field is

dark shaded, the tie-lines in the two-phase fields (bright) are schematically illustrated. See text for further details

temperature, whereas the other salt phase remains present. At this temperature, the bulk composition of this fluid inclusion is defined by mass conservation, between a brine at the cotectic curve and a solid salt phase with known composition (Fig. 11a). The intersection of this tieline with the isotherm of final dissolution of the last salt crystal finally defines the bulk composition in this ternary system (Fig. 11a) (see also Sterner et al. 1988). The trajectory of the compositional change of the brine in the halite and sylvite field is defined according to the position and orientation of tielines with increasing temperatures, and it can, therefore, not be determined exactly by purely empirical modelling. In theory, a hot KCl-rich brine in the presence of vapour precipitates a KCl-rich crystal below 600°C, $s(600)$ in Fig. 11a. The composition of the remaining brine proceeds away from $s(600)$ during further cooling, according to the orientation of the tieline at 600°C in the two-phase sylvite field. The composition of the precipitated salt crystal is slightly

enriched in NaCl during cooling, which causes the cooling trajectory of the brine to bend towards the tieline at 400°C. In other words, unlike the salt compositional changes along the cotectic curve, the salt is enriched in KCl during heating in the two-phase sylvite field.

Heide and Brückner (1967) have indicated that the change in composition of solid solutions of NaCl-rich and KCl-rich crystals is sluggish in DTA analyses with a heating rate of 4.3 °/min. Therefore, it may be expected that during a heating experiment in microthermometry, the NaCl and KCl crystals in fluid inclusions may not change their composition according to the *solvus*, but remain metastable NaCl-rich and KCl-rich solid phases (Fig. 11b). The intersection of the previously mentioned tie-line with the 600°C isotherm is substantially different from the intersection illustrated in Fig. 11a, at significant lower NaCl concentrations. Heide and Brückner (1967) also mentioned that quenched homogenous NaCl-KCl mixed crystals may exist for considerable time at temperatures below the *solvus*, and that exsolution is observed by a change in opalescence. The formation of two separated NaCl-rich and KCl-rich crystals after exsolution was not described by Heide and Brückner (1967). These metastabilities can be omitted in fluid inclusion research at low heating and cooling rates in microthermometric experiments.

Thermodynamic modelling in the ternary H₂O-NaCl-KCl system

The properties of solid solutions in binary NaCl-KCl mixtures and liquid solutions in ternary H₂O-NaCl-KCl mixtures can be described in terms of ideal solution and corresponding deviations from ideal behaviour. The equality of chemical potentials of specific components in different phases can be used to characterize the properties of these solutions (e.g. Prausnitz et al. 1986). The availability of equilibrium data of coexisting solid and liquids can be used to define the chemical potentials and to estimate its dependence on composition, temperature and pressure. Part of the ternary NaCl-KCl-H₂O fluid system, therefore, can be modelled according to these thermodynamic principles (Eqs. 13a, 13b), at conditions where a NaCl-KCl-rich brine is in equilibrium with one anhydrous salt crystal that is either rich in NaCl or KCl (*liquidus* and *solidus*), or at conditions where two solid salt crystals, i.e. a NaCl-rich and a KCl-rich phase, are coexisting (*solvus*).

$$\mu_{NaCl}^a(T, p, x) = \mu_{NaCl}^b(T, p, x) \quad (13a)$$

$$\mu_{KCl}^a(T, p, x) = \mu_{KCl}^b(T, p, x) \quad (13b)$$

where μ is the chemical potential of a component (subscript, *NaCl* and *KCl*) in a specific phase (superscript, *a* and *b*), either liquid or solid.

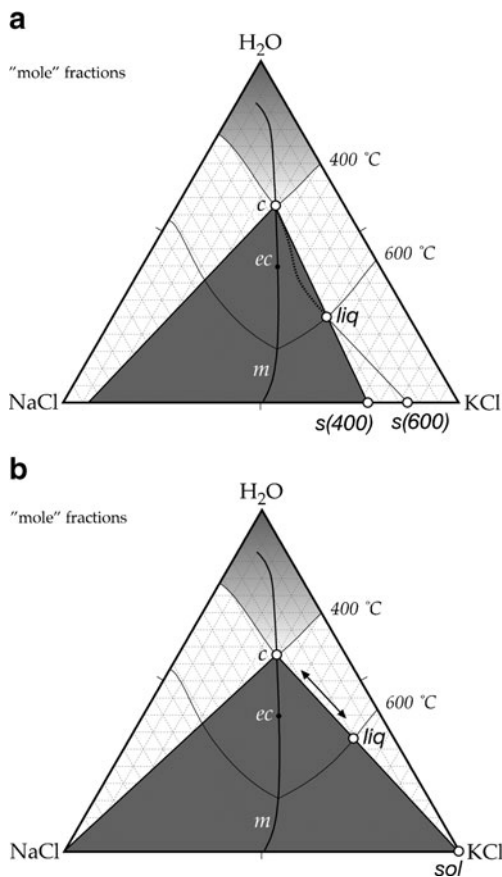


Fig. 11 a Vapour saturated *liquidus* surface in the ternary H₂O-NaCl-KCl system in “mole” fractions at 400 and 600°C. *c*=cotectic point, *ec*=end point of the cotectic curve, *m*=minimum. The three-phase field at 400°C is dark shaded. The tie-line at 600°C connects a brine (*liq*) and a solid salt phase, $s(600)$, in the two-phase fields. The open circle that is indicated with *liq* illustrates the bulk composition at final dissolution of a KCl-rich salt crystal at 600°C, whereas the NaCl-rich salt crystal already dissolved at 400°C. b Dissolution trajectory in the presence of pure NaCl and pure KCl crystals. See text for further details

In contrast to the purely empirical fitting procedures at variable pressure conditions within fluid inclusion (i.e. the *SLV* surface) described in the previous paragraphs, the temperature and composition dependency of chemical potentials are estimated at constant pressures. The chemical potential (μ) of a component (i) in a solution (*mixture*) is defined according to standard thermodynamics:

$$\mu_i^{mixture} = \mu_i^0 + RT \cdot \ln(a_i) \tag{14}$$

where R is the gas constant ($8.31451 \text{ J}\cdot\text{mol}^{-1}\cdot\text{K}^{-1}$), and a is the activity, that is defined as the product of composition (x) and activity coefficient (γ). The superscript 0 refers to the standard state, which is either the pure NaCl or pure KCl phase (Appendix B). Deviation from ideal behaviour can be expressed with the activity coefficient. The molar excess Gibbs energy (g^E) is obtained from activity coefficients of individual components according to Eqs. 15a, 15b.

$$g^E = RT \cdot \sum_i x_i \cdot \ln(\gamma_i) \tag{15a}$$

$$\left(\frac{\partial n_T g^E}{\partial n_i}\right)_{T,p,n_j} = \mu_i^E = RT \cdot \ln(\gamma_i) \tag{15b}$$

where n_T is the total amount of substance (“moles”), n_i is the amount of substance of component i and μ_i^E is the excess chemical potential of component i .

Several standard formulations of excess Gibbs energy equations are available in literature, e.g. Margules equations, Redlich-Kister expansions, or Wohl’s equations (see Prausnitz et al. 1986), which can be adapted to any solution (liquid and solid) by defining the specific interaction parameters between atoms and molecules from theoretical consideration and from experimental data. The excess Gibbs energy function for multi-component mixtures according to Wohl (1946) with simplifications (see Prausnitz et al. 1986) are used in this study to characterize solid-solutions in the binary NaCl-KCl system, and liquid-solutions in the ternary NaCl-KCl-H₂O system (Eq. 16).

$$\begin{aligned} \frac{g^E}{RT} = & q \sum_i \sum_j a_{ij} x_i x_j - 2q \sum_i a_{ii} x_i^2 \\ & + q \sum_i \sum_j \sum_k a_{ijk} x_i x_j x_k - 3q \sum_i a_{iii} x_i^3 \\ & + q \sum_i \sum_j \sum_k \sum_l a_{ijkl} x_i x_j x_k x_l - 4q \sum_i a_{iiii} x_i^4 \end{aligned} \tag{16}$$

where q is a measure of the size of the interacting molecules, a are the interaction parameters between 2, 3 and 4 molecules ($i, j, k,$ and l), which are similar to virial coefficients. Equation 16 is a general notation of the Margules equations, where the interacting molecules have similar sizes, as reflected in one q value for all components. Equation 16 can be reduced to three-suffix and two-suffix Margules equations by neglecting terms

higher than the fourth power and the third power in “mole” fractions, respectively. Occasionally, the symbol w is used (e.g. Anderson 2008) to describe non-ideal interaction behaviour between molecules that is defined by the product of the gas constant (R), temperature (in Kelvin) and the interaction parameters (qa_{ij}). Consequently, w is per definition a function of temperature. In a ternary system, the excess Gibbs energy defined in Eq. 16 can be transformed in to Eq. 17, by maximally taken into account the interaction between 3 molecules.

$$\begin{aligned} g^E = & w_{ab} \cdot x_a x_b + w_{ac} \cdot x_a x_c + w_{bc} \cdot x_b x_c + w_{aab} \cdot x_a^2 x_b \\ & + w_{abb} \cdot x_a x_b^2 + w_{aac} \cdot x_a^2 x_c + w_{acc} \cdot x_a x_c^2 + w_{bbc} \cdot x_b^2 x_c \\ & + w_{bcc} \cdot x_b x_c^2 + w_{abc} \cdot x_a x_b x_c \end{aligned} \tag{17}$$

where the subscripts $a, b,$ and c reflect the three components in the system (H₂O, NaCl and KCl). The corresponding partial molar excess Gibbs energy of a certain component (i.e. the excess chemical potential) can be obtained by using the partial differentiation as defined in Eq. 15b:

$$\begin{aligned} \mu_a^E = RT \ln \gamma_a = & w_{ab} \cdot (x_b - x_a x_b) + w_{ac} \cdot (x_c - x_a x_c) - w_{bc} \cdot x_b x_c \\ & + w_{aab} \cdot (2x_a x_b - 2x_a^2 x_b) + w_{abb} \cdot (x_b^2 - 2x_a x_b^2) \\ & + w_{aac} \cdot (2x_a x_c - 2x_a^2 x_c) + w_{acc} \cdot (x_c^2 - 2x_a x_c^2) \\ & - w_{bbc} \cdot 2x_b^2 x_c - w_{bcc} \cdot 2x_b x_c^2 + w_{abc} \cdot (x_b x_c - 2x_a x_b x_c) \end{aligned} \tag{18}$$

Solid solutions

Solid solutions at temperatures above 0°C within the ternary NaCl-KCl-H₂O system include only the components NaCl and KCl, because H₂O is not partitioned in the salt crystals. The anhydrous binary halite-sylvite system has been subject to variety of thermodynamic modelling to estimate excess Gibbs energy that defines the properties of the *solvus*, i.e. immiscibility of NaCl-rich and KCl-rich salt phases, in the range of 100 to 500°C. Three types of excess Gibbs energy equations were presented in the literature to estimate the *solvus*: 1. three-suffix Margules equation without a binary interaction parameter (Waldbaum 1969; Thompson and Waldbaum 1969) (Eq. 19a); 2. “quasi-chemical” model (Green 1970) (Eq. 19b); and 3. a partial three-suffix Margules equation (Pelton et al. 1985; Sterner et al. 1992) (Eq. 19c).

$$g^E = x_1 x_2 (x_1 W_{G2} + x_2 W_{G1}) \tag{19a}$$

$$g^E = RT \cdot \frac{Z}{2} \left[x_1 q_1 \cdot \ln \left(1 + \frac{\phi_2 (\beta - 1)}{\phi_1 (\beta + 1)} \right) + x_2 q_2 \cdot \ln \left(1 + \frac{\phi_1 (\beta - 1)}{\phi_2 (\beta + 1)} \right) \right] \tag{19b}$$

$$g^E = x_1 x_2 (x_1 w_b + w_a) \tag{19c}$$

where x_1 and x_2 are the mole fractions of NaCl (component 1) and KCl (component 2), respectively, Z (coordination number), q , ϕ , and β are defined according to Green (1970), see Eq. 20(a, b)

$$\phi_i = \frac{x_i q_i}{\sum_j x_j q_j} \tag{20a}$$

$$\beta = \sqrt{1 - 4\phi_1\phi_2 \cdot \left[1 - \exp\left(\frac{2W_G}{ZRT}\right) \right]} \tag{20b}$$

Equation 19a is a simplification of Eq. 17 by neglecting the interaction parameters between 2 molecules (a_{ij}), between 4 molecules (a_{ijkl}) and higher terms. The parameters W_{G2} and W_{G1} correspond to a_{112} and a_{122} in Eq. 16. Similarly, Eq. 19c is also a simplification of Eq. 17 by neglecting only one specific interaction parameter between 3 molecules (i.e. a_{122} in Eq. 16), and higher terms. The parameter w_a correspond to a_{12} , i.e. interaction between a NaCl and a KCl molecule, whereas the term w_b correspond to a_{112} , i.e. the interaction between two NaCl molecules and one KCl molecule.

The data of coexisting NaCl-rich and KCl-rich salt phases at 0.1 MPa from Nacken (1918), Bunk and Tichelaar (1953), Barrett and Wallace (1954) and Vesnin and Zakovryashin (1979) are used in this study to estimate best-fit values of the parameters in Eq. 19 according to the three different excess

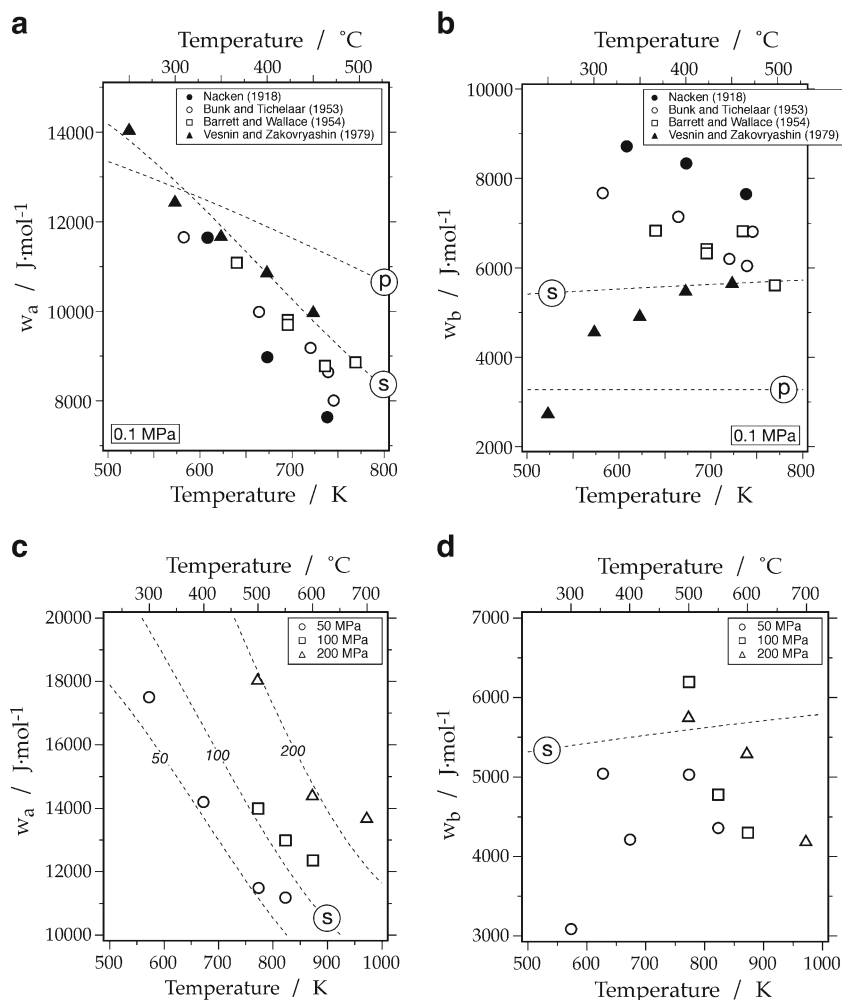
Gibbs energy definitions (see Table 9, Appendix C). Close examination of the values in Table 9 illustrates that the experimental data according to Vesnin and Zakovryashin (1970) is inconsistent to the other data sets at temperatures below 400°C. At higher pressures (up to 200 MPa), only the experimental data from Bhardwaj and Roy (1971) are used to estimate the parameters in Eq. 19.

The mathematical model used by Pelton et al. (1985) for the excess Gibbs energy (Eq. 19c) is a purely arbitrarily variation of the three-suffix Margules equation (Thompson and Waldbaum 1969, cf. Eqs. 19a and 19c). It must be noted that W_{G2} in Eq. 19a does not correspond to the same interaction parameter as w_b in Eq. 19c. This simplification does not bring any mathematical advantages, or higher accuracy in best-fit estimates. Moreover, Pelton's definitions of w_a and w_b in Eq. 19c (dashed line p in Fig. 12a and b) do not represent any of the best-fit values presented in Table 9. Sterner et al. (1992) have used the same mathematical model (Eq. 19c) to estimate the excess Gibbs energy function. The complexity of their mathematical equation that was given for w_a (see Eqs. 21 and 22 in Sterner et al. 1992) is not justified by the approximately linear distribution of best-fit values (Fig. 12a), but apparently fits to the experimental data from Vesnin and Zakovryashin (1979) (dashed line s in Fig. 12a). The coexisting values for w_b are not related to any data set (dashed line s in Fig. 12b). At high pressures (Fig. 12c and d), this model is only poorly reproducing the

Table 9 Best-fit parameters of Eq. 19 according to the experimental data of Nacken (1918, ref.1), Bunk and Tichelaar (1953, ref.2), Barrett and Wallace (1954, ref. 3), and Vesnin and Zakovryashin (1970, ref.4), at 0.1 MPa

	Temp. (°C)	x_{NaCl}^A	x_{NaCl}^B	Eq. 19a		Eq. 19b		Eq. 19c	
				W_{G1} J·mol ⁻¹	W_{G2} J·mol ⁻¹	q_1/q_2	W_G	w_a J·mol ⁻¹	w_b J·mol ⁻¹
ref. 1	335	0.98	0.12	11636.7	20347.3	0.6482	17357.0	11636.7	8710.6
	400	0.94	0.26	8969.5	17292.8	0.6493	15564.9	8969.4	8323.5
	465	0.85	0.44	7638.2	15284.8	0.6698	15137.8	7638.3	7646.5
ref. 2	309	0.979	0.111	11646.3	19310.8	0.6704	16745.6	11646.4	7664.3
	391	0.939	0.229	9986.9	17122.1	0.6841	15850.5	9986.7	7135.5
	447	0.863	0.366	9170.8	15365.5	0.7124	15307.5	9170.6	6195.0
	466	0.805	0.458	8638.8	14685.0	0.7157	15038.3	8637.8	6047.0
	472	0.809	0.479	8003.0	14802.0	0.6934	15035.7	8002.1	6800.0
ref. 3	367	0.956	0.17	11090.3	17914.6	0.6976	16363.7	11090.3	6824.2
	367	0.956	0.17	11090.3	17914.6	0.6976	16363.7	11090.3	6824.2
	422	0.904	0.291	9698.2	16098.2	0.7067	15564.9	9698.2	6400.0
	422	0.904	0.288	9787.9	16106.2	0.7096	15592.0	9788.1	6318.0
	462	0.861	0.388	8793.5	15587.0	0.6965	15459.7	8793.9	6793.0
	462	0.862	0.388	8759.3	15606.5	0.6949	15461.9	8759.4	6847.0
	496	0.708	0.564	8879.1	14465.0	0.7341	15233.3	8866.5	5600.0
ref. 4	250	0.975	0.050	14053.9	16812.7	0.8566	16399.0	14053.9	2758.7
	300	0.965	0.100	12453.9	17031.2	0.7735	16058.8	12453.9	4577.4
	350	0.945	0.155	11674.7	16616.6	0.7586	15888.7	11674.7	4942.0
	400	0.920	0.225	10877.5	16364.0	0.7396	15855.0	10877.4	5486.7
	450	0.870	0.330	9989.0	15660.0	0.7334	15665.0	9989.0	5670.9

Fig. 12 Temperature dependence of the parameters w_a **a** and w_b **b** from Eq. 18c. Individual data sets of Nacken (1918), Bunk and Tichelaar (1953), Barrett and Wallace (1954), and Vesnin and Zakovryashin (1979) are illustrated. Dashed lines p and s are the definitions according to Pelton et al. (1985) and Sterner et al. (1992), respectively. Temperature dependence of the parameter w_a **c** and w_b **d** at higher pressures (50, 100 and 200 MPa) obtained from the experimental data of Bhardwaj and Roy (1971). The dashed lines (s) represent the definition according to Sterner et al. (1992)



experimental data from Bhardwaj and Roy (1971). Any trend in the distribution of these data at various temperatures was disregarded.

The values for W_{G1} according to the model of Waldbaum (1969) and Thompson and Waldbaum (1969) are equal to those obtained for w_a (c.f. Eqs. 19a and 19c, Table 9). This thermodynamic model results in excess Gibbs energy values that are more sensitive to temperature changes than calculated with the “quasi-chemical” model (see Fig. 8 in Green 1970). However, Waldbaum’s model is unable to reproduce experimentally obtained excess enthalpy, entropy and heat capacity values (see Green 1970). In conclusion, the “quasi-chemical” model results in more accurate estimation of the non-ideal behaviour of solid solutions in the binary NaCl-KCl system than any type of the Margules equations. Therefore, the “quasi-chemical” model is adapted in this study to characterize excess Gibbs energy functions and activity coefficients. The best-fit values of the q_1/q_2 and W_G parameters obtained from experimental data are illustrated in Fig. 13 and Table 9. Similar to Fig. 12, inconsistency of several experimental data sets are exemplified in estimated q_1/q_2 values: data from Nacken (1918) systematically underestimated the values obtained

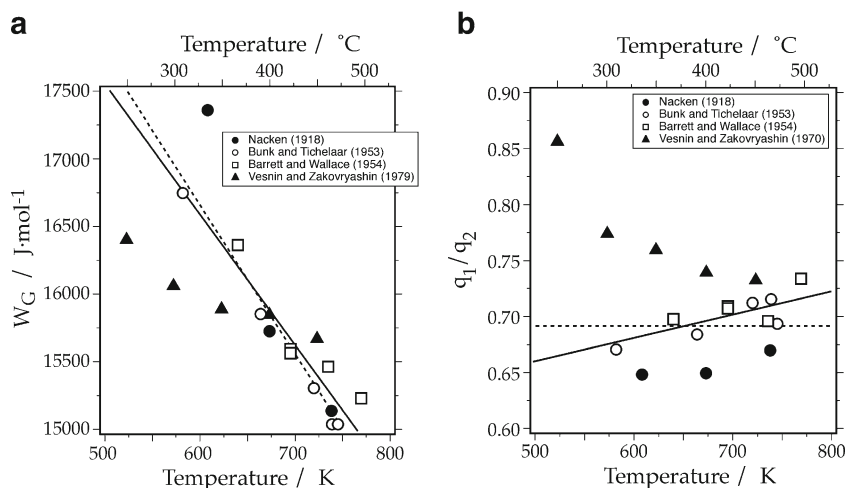
from the other data sets, whereas the values according to Vesnin and Zakovryashin (1979) are systematically overestimated, and display a reverse trend in temperature dependence. Therefore, only the data sets from Bunk and Tichelaar (1953) and Barrett and Wallace (1954) are used to estimate new linear best-fit equations in this study, which describe the temperature-dependence of both W_G and q_1/q_2 values, see Eq. 21(a, b). The pressure dependence is estimated with the data from Bhardwaj and Roy (1971)

$$W_G = 22345 - 9.5836 \cdot T + 3.5633 \cdot p \tag{21a}$$

$$\frac{q_1}{q_2} = 0.55687 + 0.00020699 \cdot T + 3.7122 \cdot 10^{-5} \cdot p \tag{21b}$$

where T is temperature in Kelvin, p is pressure in MPa. The thermodynamic definitions of W_G and q_1/q_2 and their relation to excess Gibbs energy are given by Green (1970). The amount of data does not justify polynomial fitting to higher degrees. The q_1 and q_2 values were regarded to be proportional to the molar volumes of the components (van Laar 1910) or to the atomic radii (Lumsden 1952), therefore, both temperature

Fig. 13 Temperature dependence of the parameters W_G **a** and q_1/q_2 **b** from Eq. 18b. Individual data sets of Nacken (1918), Bunk and Tichelaar (1953), Barrett and Wallace (1954), and Vesnin and Zakovryashin (1979) are illustrated. Dashed line according to Green (1970). The solid line is defined according to Eq. 21 from this study



and pressure will have a slight influence on the values of q_1 and q_2 . The best-fit equation for the ratio of q_1 and q_2 (Eq. 21b) indicates that the compressibility of NaCl is slightly higher than that of KCl. The dashed lines in Fig. 13 illustrate the values for W_G and q_1/q_2 that were defined by Green (1970), which deviate significantly from the results of this study (Eq. 21).

The maximum temperature of the *solvus* calculated with Eq. 19b and 21 is 492.6°C at 0.1 MPa and 59.21 mass% NaCl ($x_{NaCl}=0.6493$), and 504.0°C at 100 MPa and 58.85 mass% NaCl ($x_{NaCl}=0.6459$). These thermodynamically estimated values are in agreement with the value obtained at 0.1 MPa with purely empirical equations (see Eq. 11): 495.1°C and 59 mass% NaCl. This example illustrates that two purely empirical equations that contain 12 coefficients (Eqs. 11 and 12), can be reduced to 6 coefficients by using thermodynamic models (Eq. 21) without loss in accuracy. Moreover, thermodynamics allows modelling of the *solvus* at variable and higher pressures, which cannot be achieved by purely empirical modelling.

Solidus and liquidus in the binary NaCl-KCl system

At temperatures above 495°C, NaCl and KCl are completely miscible in the anhydrous solid phase. Dependent on the composition, this solid phase begins to melt at temperatures above 658°C, where the *solidus* and *liquidus* of this system are reached (e.g. Heide and Brückner 1967; Waldbaum 1969). The scatter in experimental data of *solidus* and *liquidus* (Fig. 14) illustrates the difficulty with which those data are obtained. Moreover, compositional data at constant temperatures and pressures of coexisting liquid and solid phases do not exist. In order to use equilibrium thermodynamics (see Appendix D), the composition of the solid phase that coexists with a specific known liquid phase is obtained from interpolation of data at the *solidus*. Furthermore, it is assumed that the

previously estimated excess Gibbs energy of the solid solution (Eqs. 19b and 21) is valid up to 800°C at 0.1 MPa.

The activity coefficients calculated from the experimental data of the *liquidus* from Chou (1982) and interpolated data of the *solidus* are illustrated in Fig. 15. These activity coefficients of NaCl and KCl can be reproduced by polynomial best-fits (Eq. 22).

$$\ln(\gamma_{NaCl}^{liq}) = -1.8773 \cdot (x_{KCl})^2 + 5.0682 \cdot (x_{KCl})^3 - 2.9826 \cdot (x_{KCl})^4 \tag{22a}$$

$$\ln(\gamma_{KCl}^{liq}) = -1.5656 \cdot (x_{NaCl})^2 + 4.9107 \cdot (x_{NaCl})^3 - 3.6650 \cdot (x_{NaCl})^4 \tag{22b}$$

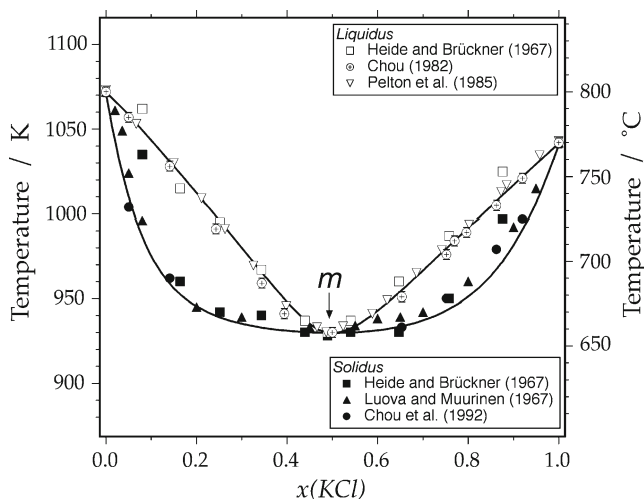


Fig. 14 *Liquidus* and *solidus* in the binary NaCl-KCl system at 0.1 MPa. “m” indicates the minimum of both curves that coincide at about $x(KCl)=0.5$. The *solidus* and *liquidus* are modelled according to equilibrium thermodynamics (Eqs. 13 and 14)

the experimental variation with temperature cannot be reproduced. However, the thermodynamically modelled position of the *liquidus* in a *Tx* diagram (see Fig. 5 in Sterner et al. 1992), is a reasonable approximation of the original experimental data (c.f. Fig. 14). This example illustrates that a large variability of activity coefficient values may result in similar calculated compositions of coexisting liquid and solid phases. This variability is due to uncertainties in properties of the *solidus*, and the previously mentioned restrictions of thermodynamic modelling.

In this study, a three-suffix Margules equation is selected to reproduce the coexisting *liquidus* and *solidus* of the binary NaCl-KCl system (line 3 *m* in Fig. 15). The experimental data that is used for the fitting procedure is the occurrence of a minimum at 658°C, 0.1 MPa and about 50 mole% NaCl (see Chou 1982), in addition to a slight asymmetry of the system. At this minimum, the composition of the liquid and solid phase is equal, which simplifies the mathematical procedure to determine the interaction parameter. At 0.1 MPa, the w_{ab} , w_{aab} and w_{abb} are defined according to Eq. 25(a, b).

$$(w_{ab} + w_{aab})/RT = -0.11267 \tag{25a}$$

$$(w_{ab} + w_{abb})/RT = -0.0365752 \tag{25b}$$

By choosing $w_{ab}/RT = -0.1$, the values of w_{aab}/RT and w_{abb}/RT are fixed at -0.01267 and 0.0634248, respectively. The complete *liquidus* and the *solidus* in NaCl-rich solution can be well reproduced with these values (see Fig. 14), whereas the *solidus* in KCl-rich solution is slightly overestimated in KCl mole fractions. The minimum is calculated at 657.9°C and 43.6 mass% NaCl (*m* in Fig. 14). By taking into account the experimental data of the minimum at higher pressures (Fig. 16), the interaction parameters are defined according to Eq. 26(a, b, c).

$$\frac{w_{ab}}{RT} = -0.1 \tag{26a}$$

$$\frac{w_{aab}}{RT} = -0.01315 - 0.0042952 \cdot p \tag{26b}$$

$$\frac{w_{abb}}{RT} = 0.062775 - 0.0049168 \cdot p \tag{26c}$$

where *p* is pressure in MPa. Similar to the considerations of Pelton et al. (1985), any temperature dependence of the parameters to define activity coefficients in the liquid solution cannot be obtained from the available experimental data.

Binary H₂O-NaCl and H₂O-KCl systems

In binary mixtures of water and salt, the excess Gibbs energy function (Eq. 17) can be mathematically reduced to a simple

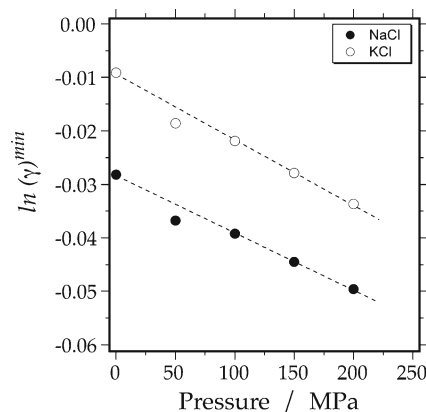


Fig. 16 Calculated activity coefficients of NaCl (solid circles) and KCl (open circles) at the minimum (see Fig. 14) and various pressures. The dashed lines are the linear best-fit equations that are used in this study

two-suffix Margules equation, by neglecting all interactions between three and more molecules. The two-suffix Margules equation with one interaction parameter (w_{ab}) theoretically provides a good representation for simple liquid mixtures, with molecules that are similar in size, shape and chemical nature. For simple systems, w_{ab} is a weak function of temperature: the value of w_{ab} frequently falls with rising temperature (e.g. Prausnitz et al. 1986). The use of this equation for binary salt-H₂O systems, which are very unlike in size, shape, and chemical nature, reduces this approach to a purely empirical mathematical best-fit procedure.

Using equilibrium thermodynamics at the *liquidus* of the NaCl-H₂O and KCl-H₂O binary fluid systems (see Eqs. 13 to 18), the interaction parameter w_{ab} can be estimated from experimental data of the dissolution temperatures of a specific salt crystal in an aqueous liquid solution (see also Sterner et al. 1992). The experimental data from Gunter et al. (1983) and Chou et al. (1992) above 400°C and 50 to 200 MPa are used in this study to estimate the interaction parameter of the *liquidus* in the NaCl-H₂O binary system (Fig. 17) and the KCl-H₂O binary system (Fig. 18), respectively. In addition, the experimental data at the *SLV* surface (Linke 1965; Sterner et al. 1988), at variable lower pressures, are also included in the fitting procedures, in order to estimate the interaction parameter at lower temperatures and pressures.

In the NaCl-H₂O system (Fig. 17), the estimated values of w_{ab} at constant pressures increase up to approximately 600°C. At higher temperatures, these values decrease rapidly, as expected from theoretical considerations of Prausnitz et al. (1986). The definitions according to Sterner et al. (1992) is similar to that of Gunter et al. (1983), and result in highly overestimated w_{ab} values at temperatures below 450°C (dashed line in Fig. 17a). The observed decrease of w_{ab} values above 600°C and pressures up to 200 MPa (dashed lines in Fig. 17b) is not reproducible with their equations that predict a continuous increase at higher temperatures.

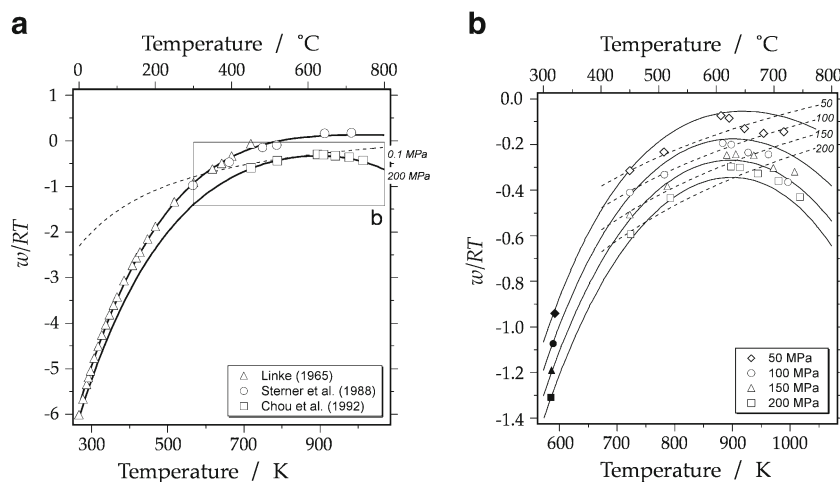


Fig. 17 Temperature and pressure dependence of the Margules coefficient w within the system $\text{H}_2\text{O-NaCl}$ in the temperature range 0 to 800°C **a** and 300 to 800°C **b**. The data obtained from Linke (1965) and Sterner et al. (1988) are illustrated in **a**, whereas the data from Chou et

al. (1992) at selected pressures are given in **b**, in addition to values calculated from Bodnar (1994) (solid symbols). The dashed lines are calculated values according to the definition of Sterner et al. (1992). The solid lines are defined according to Eq. 27 and Table 10

In the binary $\text{H}_2\text{O-KCl}$ system, the experimentally determined values of w_{ab} are highly underestimated according to Sterner et al. (1992) in the temperature range 0 to 770°C at 200 MPa (dashed line in Fig. 18a). Similarly to the $\text{NaCl-H}_2\text{O}$ system, at lower pressures down to 50 MPa and in the temperature range 400 to 800°C (Fig. 18b) calculated values according to Sterner et al. (1992) do not reproduce the experimental data. This binary system also reveals a maximum w_{ab} value around 600°C and a decrease at higher temperatures and pressures up to 200 MPa, similar to the $\text{NaCl-H}_2\text{O}$ system.

The deviation of observed *liquidus* temperatures at a selected pressure from modelled temperatures according to Eq. 27 is illustrated in Fig. 19. Most of the modelled temperatures are within 5° from experimental data in the pressure range 50 to 400 MPa, and 0.262 to 1.00 mole fraction NaCl (Fig. 19a). This deviation corresponds to 3% variation in the calculation of salinities at selected temperatures and pressures. Most of the estimated mole fractions at the *SLV* curves of both $\text{NaCl-H}_2\text{O}$ and $\text{KCl-H}_2\text{O}$ binary mixtures also deviate up to 3% from experimental data (Fig. 19b).

In this study, the w_{ab} parameter is defined as a function of temperature and pressure, Eq. 27(a, b).

$$w_{\text{H}_2\text{O-Salt}} = \sum_q W_q \cdot \tau^q \tag{27a}$$

$$W_q = w_{q0} + w_{q1} \cdot \exp(w_{q2} \cdot p) \tag{27b}$$

where τ is the temperature (in Kelvin) divided by 1000, and W_q are pressure-dependent parameters for specific water-salt

interaction, p is pressure in MPa. The values of w_{q0} , w_{q1} and w_{q2} for the binary $\text{H}_2\text{O-NaCl}$ system and $\text{H}_2\text{O-KCl}$ system are given in Table 10. It is assumed that at low temperatures the values of w_{ab} are similar in the pressure range of 0.1 to 200 MPa.

Fig. 18 Temperature and pressure dependence of the Margules coefficient w within the system $\text{H}_2\text{O-KCl}$ in the temperature range 0 to 800°C **a** and 400 to 800°C **b**. The values obtained from experimental data summarized by Chou et al. (1992) are illustrated in **b**, whereas the data from Linke (1965) and Sterner et al. (1988) are given in **a**. The dashed lines are calculated values according to the definition of Sterner et al. (1992). The solid lines are defined according to Eq. 27 and Table 10

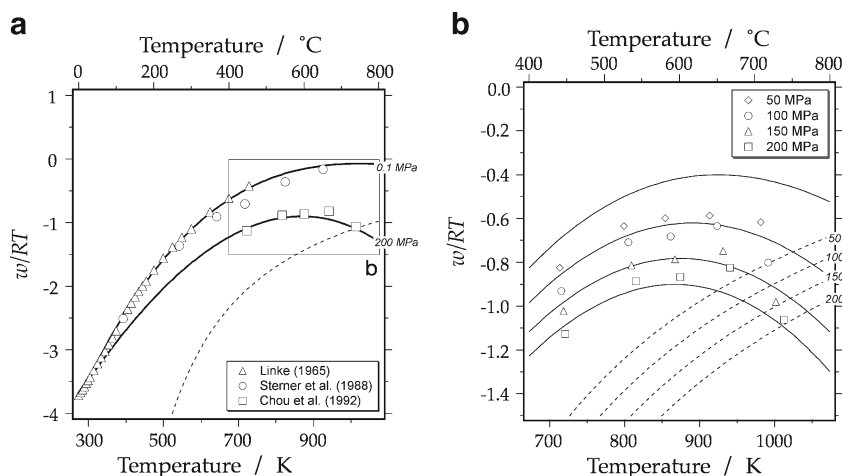


Table 10 Definition of the parameters w_{q0} , w_{q1} and w_{q2} for binary H₂O-NaCl and H₂O-KCl systems, according to Eq. 27

q	NaCl - H ₂ O			KCl - H ₂ O		
	w_{q0}	w_{q1}	w_{q2}	w_{q0}	w_{q1}	w_{q2}
0	-17.845	–	–	-3.79715	-4.59545	-0.00264824
1	64.0	–	–	-5.13472	26.5715	-0.00371846
2	-107.452	21.5378	-0.00183475	19.7843	-37.8322	-0.00224662
3	88.774	-37.146	-0.002156	-10.8436	15.7759	-0.0027738
4	-28.141	16.391	-0.00276	–	–	–

Driesner and Heinrich (2007), and it can be thermodynamically modelled according to Sterner et al. (1992). Comparison of liquidus according to these four models illustrates large differences in temperature-pressure conditions. For example, the constant slope assumption of Bodnar (1994) and the inaccurately estimated interaction parameters according to Sterner et al. (1992) may result in large deviations between experimental data and calculated liquidus (Fig. 20).

Bodnar (1994) provides the only experimental data from synthetic fluid inclusions to estimate the liquidus of a 40 mass% NaCl solution, i.e. $x(\text{NaCl})=0.1705$. The accuracy of the temperature and pressure conditions according to the equations given by Bodnar (1994) of this liquidus depends very much on the “graphical smoothing” of experimental data, in addition to variation in homogenisation temperatures T_h (SLV→SL) and dissolution temperatures T_m (SL→L). These experiments illustrate a relationship between T_h and

experimental conditions (T_{exp} and p_{exp}). Isobars of equal experimental pressures are defined in a T_h - T_{exp} diagram (Fig. 20a) according to Eq. 28(a, b, c):

$$T_h(\text{SLV} \rightarrow \text{LV}) = m + n \cdot T_{\text{exp}} \quad (28a)$$

$$m = 56.299 - 0.36766 \cdot p_{\text{exp}} + 0.00027398 \cdot p_{\text{exp}}^2 \quad (28b)$$

$$n = 0.82248 - 0.00051484 \cdot p_{\text{exp}} \quad (28c)$$

where T_{exp} and p_{exp} are the experimental temperature (in °C) and pressure (in MPa), respectively. This equation corresponds to the “graphically smoothed” part of data treatment that was not mathematically specified by Bodnar (1994). The coexisting T_m values correspond to minimum experimental temperatures, which can also be projected in Fig. 20a (triangles). Subsequently, the pressure at T_m (i.e. the liquidus) can be directly obtained from Eq. 28. The calculated pressures at the liquidus display a non-linear distribution (Fig. 20b), in contrast to the constant-slope assumption of Bodnar (1994) (line *b94* in Fig. 20b). Experimental data above 200 MPa were rejected by Bodnar (1994) because stretching of inclusions was expected due to high internal pressures at liquidus temperatures. However, quartz is not likely to deform in an elastic mode at temperatures around 315°C, but internal overpressures may generate micro-cracks (brittle deformation) that will cause inclusions to leak their fluid contents completely. These inclusions are easily recognized by the absence of fluid after the experimental heating run.

The difference between the four models can be best illustrated with two examples based on two types of experimental data: **a.** 40 mass% NaCl solution (Fig. 20b) with synthetic fluid inclusions (Bodnar 1994); and **b.** 76.4 mass% NaCl solution (Fig. 20c) with DTA analyses (Gunter et al. 1983). At the SLV curve of the binary NaCl-H₂O system, a 40 mass% NaCl solution in fluid inclusions result in an equal T_m and T_h value at 329°C according to this study, whereas 323°C is predicted by Bodnar (1994) and 328°C by Driesner and Heinrich (2007) (Fig. 20b). The purely empirical equation according to Sterner et al. (1988) results in a temperature of 325°C. The thermodynamic model according to Sterner et al. (1992) results in a highly overestimated T_h value at 366°C (not

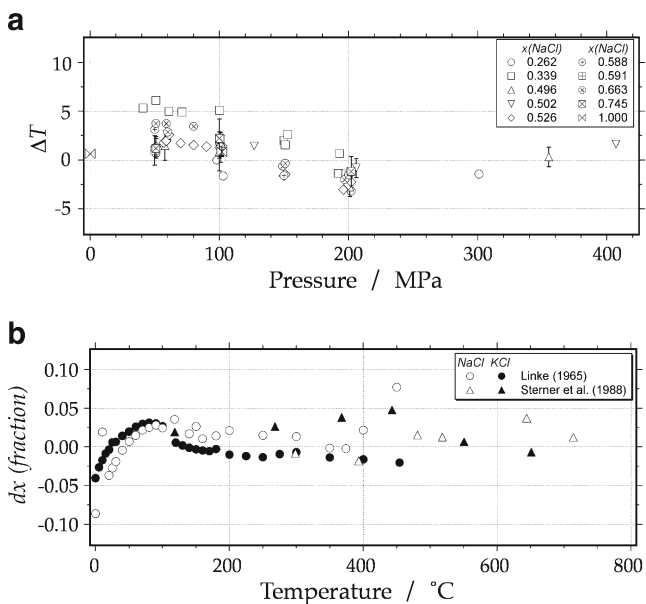


Fig. 19 **a** Deviations in dissolution temperatures (ΔT) obtained from thermodynamic models (Eq. 27) and experimental data (Gunter et al. 1983) in the binary H₂O-NaCl system. **b** Deviations in salinity calculations (dx) between thermodynamic models (Eq. 27) and experimental data from Linke (1965) and Sterner et al. (1988) along the SLV curves of the binary H₂O-NaCl system and H₂O-KCl system

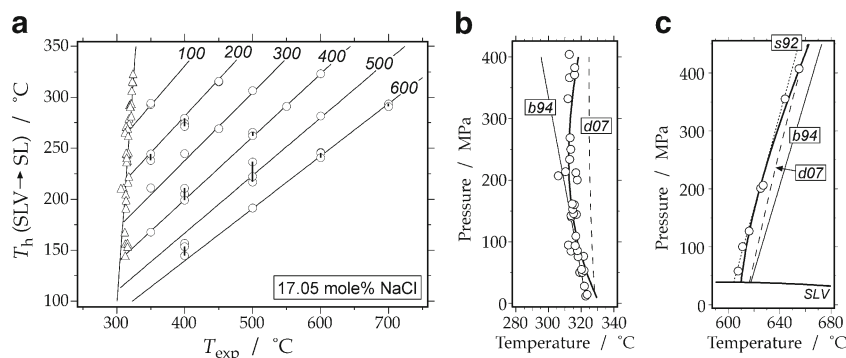


Fig. 20 a Experimental method to estimate the pressure in fluid inclusions at *liquidus* conditions in a $T_h - T_{exp}$ (i.e. experimental temperature) diagram with isobars (in MPa). See text for further details. Calculated *liquidus* of a $x(\text{NaCl})=0.1705$ solution (40 mass%

NaCl) **b** and a $x(\text{NaCl})=0.5$ solution (76.4 mass% NaCl) **c**, according to Bodnar (1994) (b94), Sterner et al. (1992) (s92), and Driesner and Heinrich (2007) (d07), with experimental data from Bodnar (1994) (open symbols)

illustrated in Fig. 20b). At 400 MPa, the constant slope model according to Bodnar (1994) results in highly underestimated temperatures (around 295°C) compared to experimental data and calculations from this study (around 317°C). The nearly constant slope *liquidus* according to Driesner and Heinrich (2007) is overestimating experimental temperatures up to 400 MPa. The thermodynamically modelled *liquidus* in this study according to Eq. 27 (thick curve in Fig. 20b) is able to reproduce the experimental data and a variable slope up to 400 MPa.

inclusions from $T_h(\text{SLV} \rightarrow \text{SL})$ and $T_m(\text{SL} \rightarrow \text{L})$ values. They added an unknown amount of “excess” halite to a saturated liquid solution at room temperature, which however does not guarantee the presence of a solid halite phase at high experimental temperatures and pressures. The heterogeneity of the experimentally obtained inclusions was not investigated in that study, and T_m values may reflect increased salinities due to accidentally trapped halite crystals during the experiment. The equation given by Becker et al. (2008) can reproduce approximately the *liquidus* of the 40 mass% NaCl solution estimated by Bodnar (1994) up to 250 MPa. At higher pressures, this equation becomes increasingly inaccurate.

In a 76.4 mass% NaCl aqueous solution, i.e. $x(\text{NaCl})=0.502$, the experimental data from Gunter et al. (1983) are well reproduced by the thermodynamic models according to Sterner et al. (1992) and this study, whereas Bodnar (1994) and Driesner and Heinrich (2007) predict higher temperatures (Fig. 20c). At the *SLV* curve, the latter predicts a T_h value of 616°C, whereas the extrapolated DTA analyses according to the thermodynamical model from Sterner et al. (1992) predicts 604°C, and this study results in a temperature of 610°C. At higher pressures, both thermodynamic models are increasingly different. For example, the experimental pressure of the *liquidus* at 655°C is 407 MPa (see Gunter et al. 1983). The calculated pressure according to Sterner et al. (1992) is 455 MPa, and 314 MPa according to Bodnar (1994), whereas this study predicts a pressure of 403 MPa. The purely empirical model from Driesner and Heinrich (2007) approaches the thermodynamic models at higher pressures.

Liquid solution in the ternary H₂O-NaCl-KCl system

Within the *SL* field and at *liquidus* conditions (e.g. Fig. 1), the NaCl-H₂O system consists of a saturated brine in the presence of solid NaCl crystals. Consequently, trapping this fluid in quartz results in the formation of fluid inclusions with a variety of salinities because small crystals of halite may be accidentally trapped in a number of inclusions, whereas the majority of the inclusions will trap only a saturated solution. Becker et al. (2008) have used this technique in semi-controlled experiments with unknown compositions to obtain a mathematical model to calculate minimum trapping pressures of

The three-suffix Margules equation (see also Eq. 17) contains one parameter that describes the non-ideal behaviour of the interaction between three different molecules, i.e. H₂O, NaCl and KCl. This parameter can be estimated from experimental data in the ternary system. However, the accuracy of the values of this parameter is highly dependent on the previously thermodynamically modelled interaction parameters between two molecules, i.e. NaCl-KCl, NaCl-H₂O, and KCl-H₂O.

At the *SLV* surface, experimental data in the ternary system are available at variable pressures from Sterner et al. (1988) and Linke (1965). At higher and constant pressures, Chou et al. (1992) provides the only data set in this ternary system at 50, 100, 150 and 200 MPa. This data set includes only the composition of a liquid solution and the temperature of the *liquidus*, whereas the composition of the coexisting solid phase is unknown. In order to apply equilibrium thermodynamics to calculate the ternary parameter in Eq. 17, the composition of coexisting solid solutions has to be known. However, H₂O is completely excluded from the solid salt phase, therefore, the available information can be used to calculate simultaneously the composition of the coexisting solid phase and the ternary interaction parameter w_{abc} in the

liquid phase (see Table 11 in ESM for compositional data). The calculated values for w_{abc} reveal a significant amount of scatter at variable temperatures and pressure (Fig. 21a). The experimental precision of the temperature measurement in the DTA method (e.g. Chou 1982) is about 3° at its best. Consequently, the variation in the calculated value of w_{abc}/RT that is caused by this precision is about 0.3 at relative low temperatures, but increases up to 4 at high temperatures. Variations in w_{abc}/RT up to 6 can be expected from a precision of 5° in DTA temperature measurements. The w_{abc}/RT values increase at higher temperatures and pressures, and they are best reproduced by a polynomial function (Fig. 21b, Eq. 29a, b, c, d).

$$\frac{w_{abc}}{RT} = \sum_i s_i \cdot T^i \quad (29a)$$

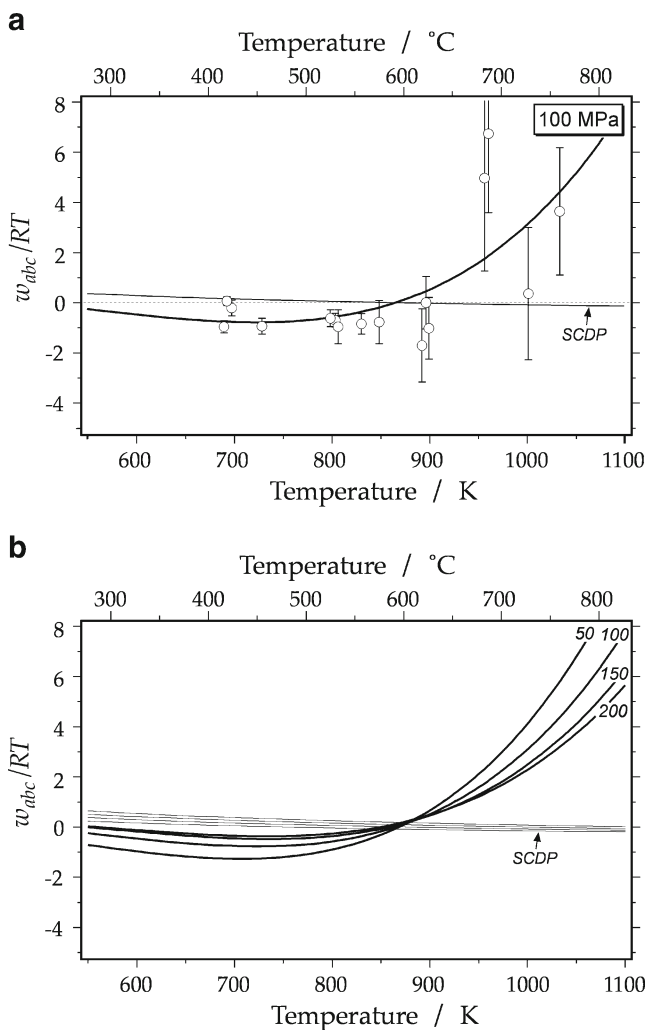


Fig. 21 Dimensionless ternary interaction parameter w_{abc}/RT as a function of temperature and pressure. **a** Variation due to the precision in temperature measurements from the DTA at 100 MPa. The SCDP curve is calculated with the equations from Sterner et al. (1992). **b** The effect of pressure, i.e. 50, 100, 150, and 200 MPa on the w_{abc}/RT parameter

$$s_2 = [17.126 + 0.04484 \cdot p - 0.00024 \cdot p^2] \cdot 10^{-6} \quad (29b)$$

$$s_3 = [-73.651 + 0.12442 \cdot p] \cdot 10^{-9} \quad (29c)$$

$$s_4 = [62.064 - 0.20174 \cdot p + 0.0003211 \cdot p^2] \cdot 10^{-12} \quad (29d)$$

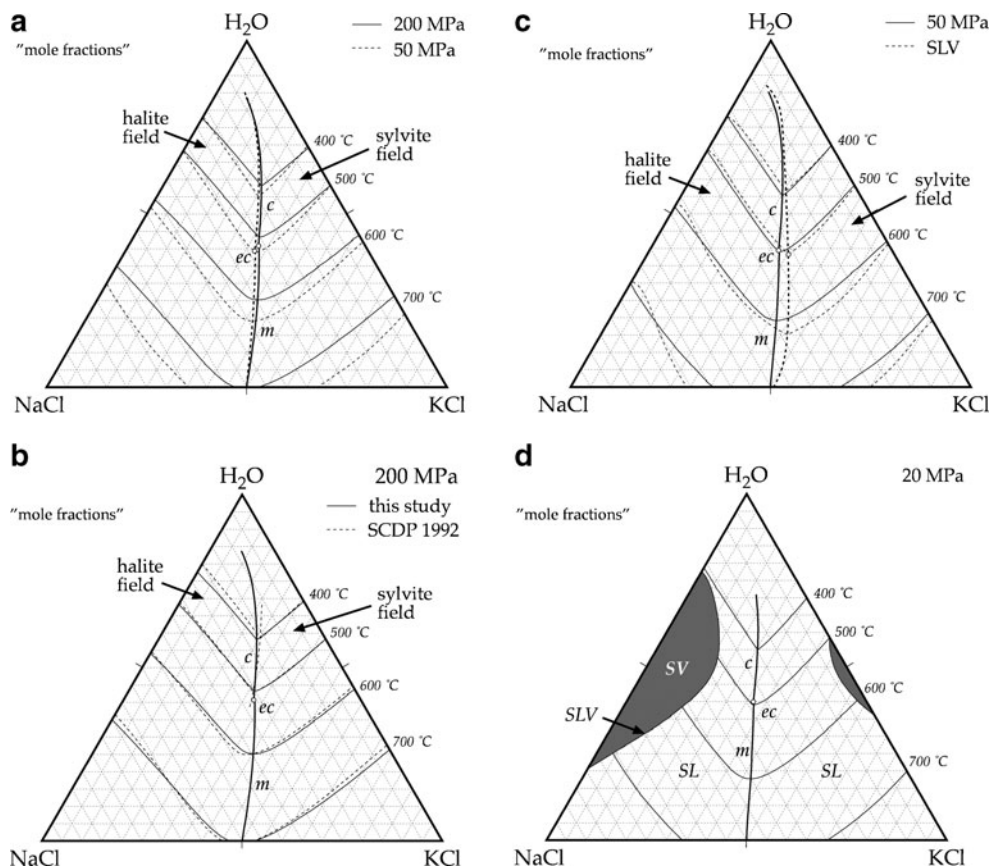
where T is the inverse of temperature (in K), and p is pressure (in MPa), the value of i varies from 2 to 4. The w_{abc}/RT values modelled with the definitions from Sterner et al. (1992) are approximately zero, and do not influence the non-ideal behaviour in ternary mixtures (Fig. 21). Moreover, they predict a decreasing w_{abc}/RT value with increasing temperature, in contrast to the trend of experimental data, whereas uncertainty analyses were excluded.

Isotherms, cotectic curve, minimum curve and tie-lines of the thermodynamically modelled liquidus at constant pressures

The thermodynamic model presented in the previous paragraphs can be used to calculate isotherms of the liquidus in the compositional triangular diagrams of the H₂O-NaCl-KCl system (Fig. 22). With decreasing pressures, isotherms shift towards the base (NaCl-KCl) of the diagram (Fig. 22a). The cotectic line is calculated from the equality of chemical potentials of a liquid phase, a NaCl-rich solid salt phase, and a KCl-rich solid salt phase (see Eq. 13), and is also displayed in Fig. 22. The end-point of the cotectic line (*ec* in Fig. 22a) is calculated at 498.3°C at 50 MPa, and 515.4°C at 200 MPa and nearly equal total compositions. At higher temperatures, the boundary between NaCl-rich and KCl-rich ternary systems can be defined by the minimum (line *m* in Fig. 22a, see also Fig. 9). It should be noted that the starting point of the minimum line does not coincide with the end-point of the cotectic line, and these curves are discontinuous. The cotectic and minimum lines are shifted slightly to KCl-richer compositions at higher pressures.

Isotherms, cotectic line and minimum line calculated with the thermodynamic model according to Sterner et al. (1992) are only slightly different from this study (Fig. 22b), which illustrates that a similar liquidus surface in the ternary H₂O-NaCl-KCl system can be obtained from completely different estimated non-ideal interaction parameters (w) due to the multiple correction procedures. In other words, highly overestimated w -values in binary H₂O-salt systems subsequently result in highly underestimated w -values in ternary H₂O-salts systems, in order to reproduce the same liquidus surface. However, the individual values of the w parameters are completely meaningless, and do not represent true non-ideal behaviour. Large deviations between

Fig. 22 Liquidus surface in the ternary H₂O-NaCl-KCl system in “mole” fractions according to thermodynamic modelling at constant pressures with isotherms, cotectic-line (*c*) cotectic end point (*ec*) and minimum (*m*). **a** at 50 and 200 MPa. **b** comparison at 200 MPa with the model according to Sterner et al. (1992) (abbreviated with *SCDP* 1992). **c** comparison between the thermodynamic model at 50 MPa and the purely empirical model of the *SLV* surface. **d** the liquidus at 20 MPa with the intersection of the *SLV* surface and the occurrence of two *SV* fields are shown



these thermodynamic models occur at temperatures below 450°C (Fig. 22b), where the liquidus in the halite field is located at higher H₂O contents (up to 3 absolute mole%) than this study. The position of the cotectic line is increasingly deviating from this study at lower temperatures, whereas the minimum-line was not defined by Sterner et al. (1992).

A comparison of the thermodynamic model at 50 MPa with the purely empirical model at the *SLV* surface (at variable pressures) that is presented in the first part of this study is illustrated in Fig. 22c. The position of isotherms based on the two types of modelling is approximately consistent. For example, the 600°C isotherm in the sylvite and halite field of the *SLV* surface shift towards the NaCl-KCl base at intermediate compositions, which corresponds to the shift according to decreasing pressure in the thermodynamic model (c.f. Fig. 22a). The cotectic and minimum line at the *SLV* surface deviate from the thermodynamically determined curves, and are located at higher relative KCl compositions (up to 5 absolute mole%).

At 20 MPa, the *SLV* surface intersects with the calculated isotherms in the *SL* field (Fig. 22d), and two *SV*-fields (solid+vapour) occur in the diagram, which include a saturated vapour-like brine in equilibrium with either NaCl or KCl. The continuation of isotherms inside these fields is unknown due to the lack of experimental data.

The purely empirical model from the first part of this study is able to predict the *SLV* surface and immiscibility of a solid anhydrous salt phase up to 495°C. The thermodynamic model gives a complete reproduction of the H₂O-NaCl-KCl system, including liquidus, solidus and the anhydrous solvus up to 400 MPa. The latter model can, therefore, reproduce tielines between a brine and a solid salt phase in thermodynamic equilibrium at selected pressures and temperature. For example, at 700°C and 50 MPa (Fig. 23a), a brine highly enriched in NaCl is in equilibrium with a solid salt crystal with a “mole” fraction of NaCl between 0.87 (point salt in Fig. 23a) and 1. At 600°C (Fig. 23b), the composition of the solid salt phase in equilibrium with a specific brine is a continuous range between pure NaCl and KCl. For example, a fluid inclusion with a salt crystal of composition s_{KCl} (see Fig. 23b) is in equilibrium with a brine of composition *liq* (see Fig. 23b), in the absence of a vapour phase. At 400°C (Fig. 23c), the anhydrous NaCl-KCl phase is exsolved in a NaCl-rich and a KCl-rich salt phase that causes the occurrence of a three-phase field. At these conditions, a fluid inclusion contains the phase assemblage of a brine at the cotectic line (point *c* in Fig. 23c), a NaCl-rich salt cube (s_{NaCl} in Fig. 23c), and a KCl-rich salt-cube (s_{KCl} in Fig. 23c), in the absence of a vapour phase. Outside this sub-triangle, tielines can be determined between a brine and a NaCl-rich crystal, or between a brine and a KCl-rich crystal.

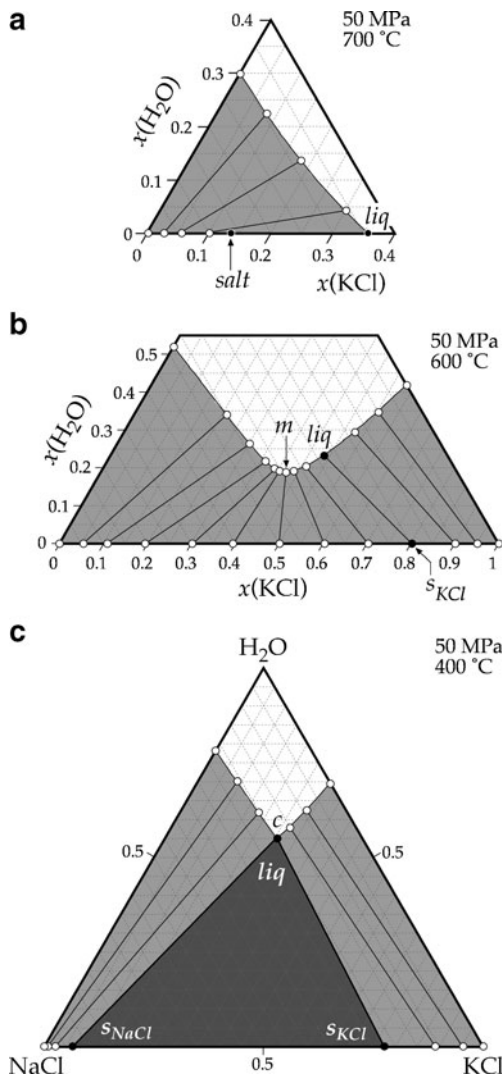


Fig. 23 Calculated tielines at the *liquidus* surface in the ternary H₂O-NaCl-KCl system in “mole” fractions according to thermodynamic modelling at 50 MPa and **a** 700°C; **b** 600°C; and **c** 400°C

Conclusions

A H₂O-NaCl-KCl-rich fluid occurs occasionally in fluid inclusions in a variety of geological environments. The properties of this fluid provide information about the conditions of entrapment, and thereby, conditions that have affected the rock. This fluid system has already been studied extensively and modelled according to thermodynamic principles and purely empirical “best-fit” analyses. However, the provided models are internally inconsistent and are partly not reproducing accurately the available experimental data. Interaction parameters in thermodynamic models were poorly defined and are not consistent with activity coefficients obtained from experimental data.

New polynomial best-fit equations are developed for isotherms and isobars of the H₂O-NaCl-KCl *liquidus* in the hydrohalite-field, the halite-field, and the sylvite-field, in the

presence of a vapour phase (the *SLV* surface). The anhydrous *solvus* of the NaCl-KCl system is modelled with new polynomial fittings at 0.1 MPa.

The excess Gibbs energy of the *liquidus*, *solidus* and *solvus* in the ternary H₂O-NaCl-KCl system is thermodynamically modelled according to Margules equations at selected constant pressures (the *SL*-surface). Interaction parameters of the NaCl-KCl solid solution are obtained from the *solvus* at a variety of pressures, using the “quasi chemical” model. Interaction parameters of the liquid solution of the NaCl-KCl system are obtained from the coexistence of *liquidus* and *solidus* up to 200 MPa and 900°C. Interaction parameter for the binary H₂O-NaCl and the binary H₂O-KCl system are modelled according to a two-suffix Margules equation up to 400 MPa. The parameter that describes the interaction between H₂O, NaCl and KCl is obtained from a three-suffix Margules equation.

These models are included in the software package *FLUIDS* (Bakker 2003), to apply directly the mathematical functions in fluid inclusion studies and in general fluid properties investigations. The computer program *AqSo WHS* has been developed in REALBasic (© Real Software, Inc.) with a graphical user interface. The program is composed of four main applications: 1. salinity determination from known dissolution temperatures, at variable pressure (*SLV*) and constant pressures (*SL*); 2. dissolution temperature determination from known salinities at variable pressures (*SLV*) and constant pressures (*SL*); 3. determination of the anhydrous *solvus*; 4. determination of the cotectic and minimum lines in the ternary compositional diagram of the H₂O-NaCl-KCl system

Acknowledgement I greatly acknowledge the comments of two anonymous reviewers

Appendix A

Computer program AqSo WHS

The computer package *FLUIDS* was presented by Bakker (2003) to analyse fluid properties in rock pores and in inclusions within crystals. This package includes the series of “*AqSo*” programs that can be used to calculate the properties of salt-bearing aqueous fluids in fluid inclusions. This series was originally designed with a SIOUX interface (Simple Input/Output User Exchange). The new program *AqSo WHS* (Fig. 24) is added to this series and uses both the purely empirical and thermodynamic models of the H₂O-NaCl-KCl fluid systems that are presented in this study. The new program is provided with a Graphical User Interface (GUI, REALBasic 2009). The program includes the calculation of salinities from known dissolution temperatures and pressures, in addition to the calculation of dissolution temperatures and pressures from known salinities (Fig. 25).

Fig. 24 The “Start” window of the program *AqSo WHS*, indicating that a purely empirical model and a thermodynamic model are used to calculate fluid properties in the fluid system $\text{H}_2\text{O}-\text{NaCl}-\text{KCl}$ according to the considerations of this study. It also illustrates a three-phase (*SLV*) fluid inclusion at room temperature

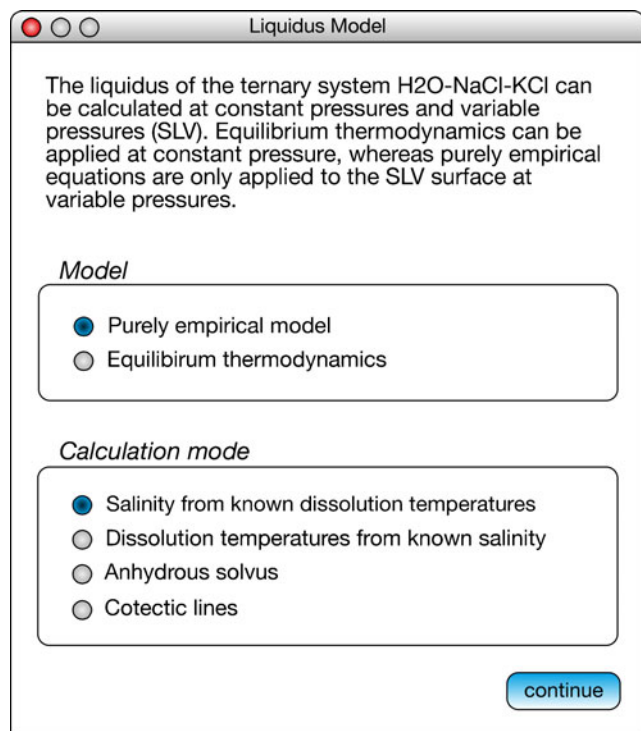
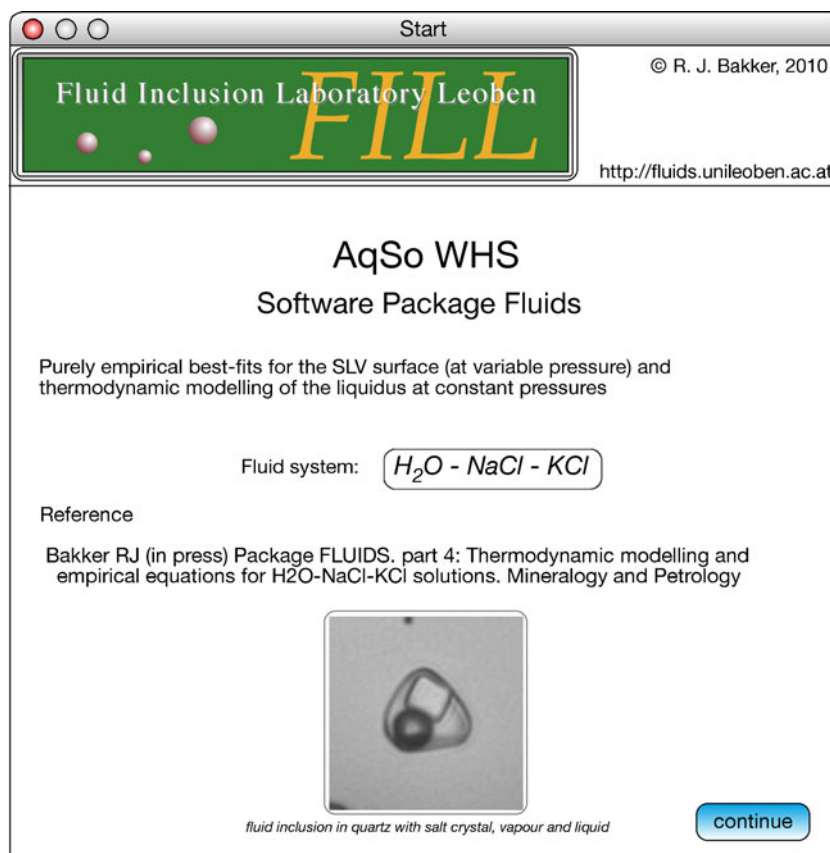


Fig. 25 The “Liquidus Model” window of the program *AqSo WHS* in which the purely empirical model or an equilibrium thermodynamic model can be selected, in addition to a specific calculation procedure

Furthermore, chemical potentials and activities of NaCl and KCl can be calculated at selected temperatures and pressures. The program has been compiled for three different computer operating systems: Mac OS X (PowerPC and Intel coprocessor), Microsoft Windows (2000, XP, Vista, 7) and Linux (GTK+2.x), and it can be downloaded from the *FILL* (Fluid Inclusion Laboratory Leoben) website: <http://fluids.unileoben.ac.at/Computer.html>

A calculation example using purely empirical equations (Eqs. 2 to 12) is illustrated in Fig. 26. In a microthermometric experiment, a halite and sylvite crystal dissolve in the aqueous solution in a fluid inclusion (“dissolving phases” in Fig. 26). The program gives automatically the temperature limits, between which these crystals may theoretically dissolve in the solution. The dissolution temperature of halite and sylvite are separately introduced and the salinities can be calculated, by using the push-bottom “calculate” (see Fig. 26). The results of the calculation are given within the sub-window “Properties of liquid solution” (Fig. 26). The cotectic is defined by the dissolution of the first salt crystal, i.e. sylvite, at 393.15 K (120°C). At this temperature, the aqueous liquid solution contains 6.96 mole% NaCl and 8.55 mole% KCl (amount of substance—as—fractions). Expressed in mass fractions: $w(\text{NaCl})=15.85\%$ and $w(\text{KCl})=24.85\%$ (the remaining fraction is assigned to H_2O). Furthermore, the remaining anhydrous salt crystal has a composition of $x(\text{NaCl})=0.9973032$ at this

Fig. 26 The calculation procedure “SLV surface H₂O-NaCl-KCl” to calculate NaCl and KCl salinities from dissolution temperatures, according to the purely empirical model. See text for further details

SLV surface H₂O-NaCl-KCl

Purely empirical model (variable pressure)

Salinity calculations from known temperatures

Dissolving Phases

- Ice + Hydrohalite
- Ice + Sylvite
- Hydrohalite + Halite
- Hydrohalite + Sylvite
- Halite + Sylvite

Temperature limits of dissolution

Limits cotectic line: from -2.3 to 658 °C
 Halite dissolution: -2.3 to 658-801 °C
 Sylvite dissolution: -2.3 to 658-770 °C

phase diagram

Dissolution Temperatures:

Ice °C
 Hydrohalite °C
 Sylvite °C
 Halite °C

Properties of liquid solution

	Cotectic	Final Dissolution
Temperature	393.15 K	573.15 K
Pressure	low value	4.909829 MPa
as%* NaCl	6.958609	12.37787
KCl	8.553146	12.05748
mass% NaCl	15.84972	24.24986
KCl	24.84965	30.13113

Composition remaining solid at cotectic temperature: salt, $x(\text{NaCl}) = 0.9973032$

as% = amount-of-substance percentage ("mole" percentage)

temperature. At the final dissolution temperature 573.15 K (300°C) of the NaCl-rich halite crystal the remaining aqueous liquid solution contains 24.25 mass% NaCl and 30.13 mass% KCl (Fig. 26). The program gives up to 6 decimal places of calculated values according to the algorithms. The number of decimal place of real temperatures and compositions are restricted by analytical techniques to measure these parameters, therefore, the numbers in Fig. 26 have to be rounded to one decimal for temperature (T), four decimals for the fraction in composition (x), and two decimal for a fraction expressed in percentage. The number of decimal places is defined by the uncertainty of the analytical technique.

A second example of the program *AqSo WHS* is illustrated in Fig. 27, using the thermodynamic model of the H₂O-NaCl-KCl system (Eqs. 13 to 29). The pressure is defined at 100 MPa, and the composition of the system is introduced in mass% NaCl and KCl. The program also offers the possibility to introduce compositions in “mole” percentage or molalities. The given composition is recalculated in each of these quantities. The thermodynamic modelling can only be applied to the halite-

and sylvite field, which have to be selected according to the given bulk composition of the fluid system (Fig. 27). The final dissolution temperature 129.0°C of the salt crystal (in this case halite) is calculated by using the push-bottom “calculate” (see Fig. 27). The program also gives the activity of both NaCl and KCl in the aqueous liquid solution at this temperature, and the composition of the NaCl-rich halite crystal, $x(\text{NaCl}) = 0.9997371$. The pressure of the *SLV*-surface is also given for comparison with the purely empirical model (Eqs. 2 to 12). In this example it is illustrated that this pressure is lower than 1 MPa, and not precisely defined according to the empirical equations.

Appendix B

Standard state

The standard state chemical potential of NaCl and KCl in both liquid and solid solutions (Eq. 14) is chosen as the pure NaCl

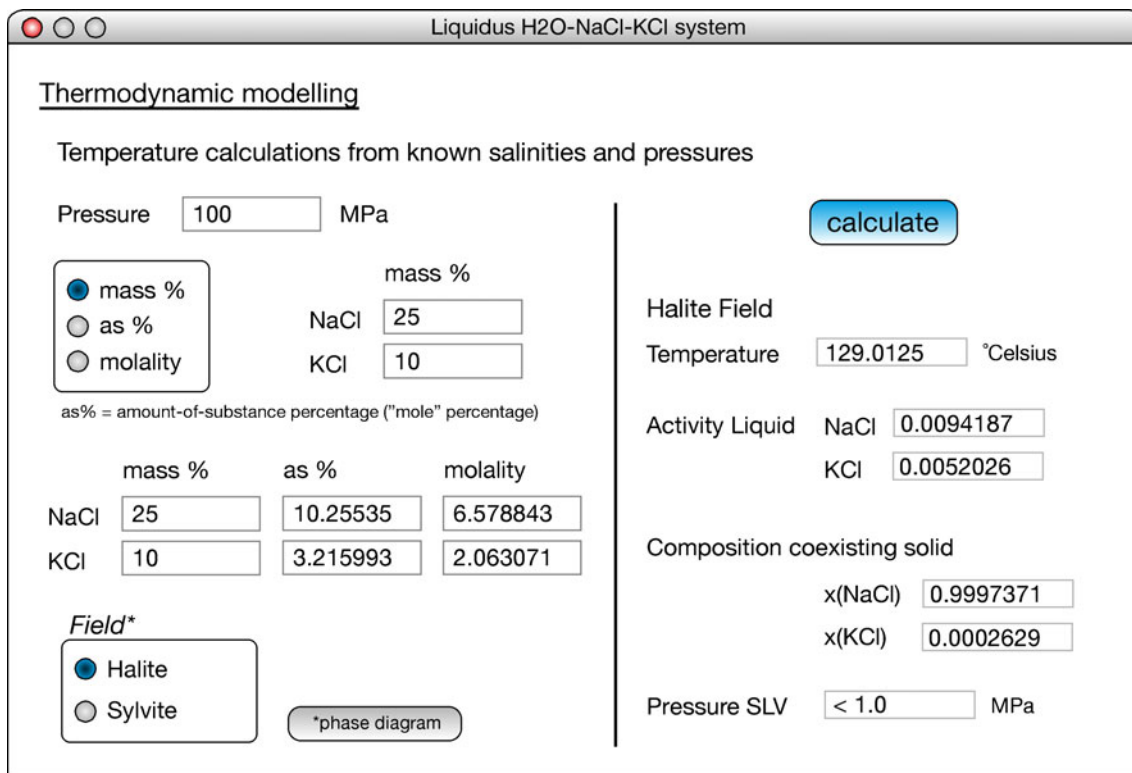


Fig. 27 The calculation procedure “Liquidus H₂O-NaCl-KCl system” to calculate the final dissolution temperature of a salt crystal from known NaCl and KCl salinities. See text for further details

and pure KCl phases. Consequently, the equality of chemical potentials of NaCl in liquid and solid solutions (Eq. 13) includes the definition of the melting of pure NaCl. Similarly, the melting of pure KCl is also included in the equality definition. The properties of the melting of pure phases is defined by standard thermodynamics (Eqs. B1 to B5)

$$\Delta\mu_i^{melt} = (\mu_i^0)^{liquid} - (\mu_i^0)^{solid} \quad (B1)$$

$$\Delta\mu_i^{melt} = \Delta H_i^{melt} - T_m \cdot \Delta S_i^{melt} + \Delta V_i^{melt} \cdot (p - 0.1) \quad (B2)$$

$$\Delta H_i^{melt} = \Delta H_i^{melt}(T_m) + \int_{T_m}^T \Delta C_{P_i}^{melt} dT \quad (B3)$$

$$\Delta S_i^{melt} = \Delta S_i^{melt}(T_m) + \int_{T_m}^T \frac{\Delta C_{P_i}^{melt}}{T} dT \quad (B4)$$

$$\Delta C_{P_i}^{melt} = (C_{P_i})^{liquid} - (C_{P_i})^{solid} \quad (B5)$$

where ΔH , ΔS , ΔV and ΔC_P are the enthalpy, entropy, volume, and heat capacity of melting, respectively. T_m is the melting temperature of a pure salt at 0.1 MPa. The entropy of melting at 0.1 MPa is directly obtained from the enthalpy of

melting (Eq. B6). The volume of melting is obtained from the Clapeyron equation (Eq. B7)

$$\Delta S_i^{melt}(T_m) = \frac{\Delta H_i^{melt}(T_m)}{T_m} \quad (B6)$$

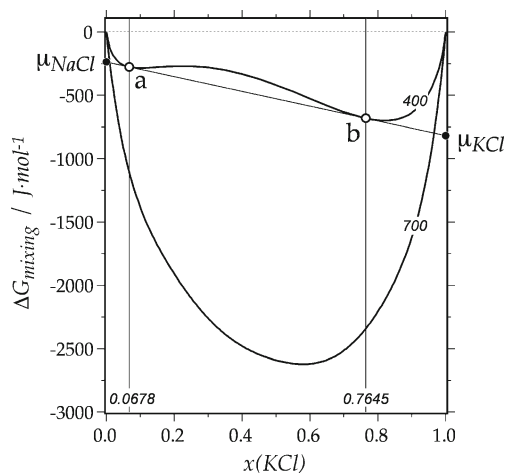


Fig. 28 ΔG_{mixing} - x diagram at 0.1 MPa for the solid solution of NaCl and KCl, at 400°C and 700°C. The composition of coexisting immiscible solid phases **a**, $x(KCl)=0.0678$, and **b**, $x(KCl)=0.7645$, are defined by a common tangent at 400°C. See text for further details

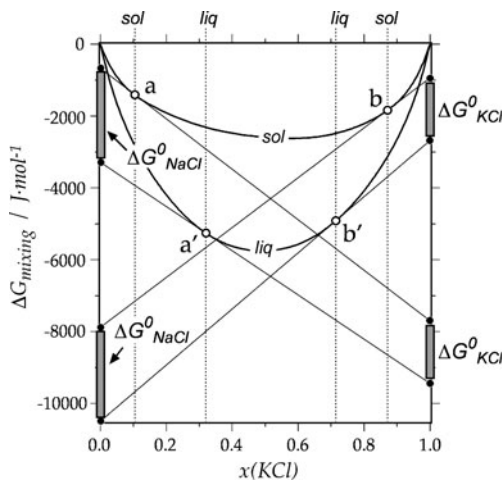


Fig. 29 $\Delta G_{mixing}-x$ diagram at 0.1 MPa for the solid (sol) and liquid (liq) solution of NaCl and KCl at 700°C, which define the coexisting solidus and liquidus. ΔG_{NaCl}^0 and ΔG_{KCl}^0 are the Gibbs energy change of the melting of pure NaCl and KCl, respectively. See text for further details

$$\Delta V_i^{melt} = \left(\frac{dT}{dp} \right) \cdot \Delta S_i^{melt} \quad (B7)$$

The heat capacity of pure NaCl in the liquid and solid phase is obtained from Robie et al. (1979). The melting temperature of pure NaCl at 0.1 MPa is 1073.8 K, and the enthalpy of melting of pure NaCl is 28158 J·mol⁻¹ (Robie et al. 1979). The slope of the NaCl melting curve in a pT diagram is obtained from Chou (1982). The heat capacity of pure KCl in the solid phase is obtained from Robie et al. (1979). The heat capacity in the liquid phase is defined by Chase et al. (1985). The melting temperature of pure KCl at 0.1 MPa is 1043 K and the enthalpy of melting is 26284 J·mol⁻¹ (Robie et al. 1979). The slope of the KCl melting curve in a pT diagram is obtained from Chou (1982).

Appendix C

Determination of the interaction parameters w in NaCl-KCl solid solutions

Experimental data of the solvus in the anhydrous NaCl-KCl system, i.e. coexisting NaCl-rich salt phase and KCl-rich salt phase, can be used to estimate some of the interaction parameters in Eqs. 16 and 17. At equilibrium, the chemical potentials of NaCl and KCl must be equal in both coexisting solid phases (see Eq. 13). The standard state chemical potential for both phases are the pure end-members, which is, therefore, eliminated in the equality equations. The resulting equations include the equality of the activities of NaCl in both solid phases, and the equality of the activities of KCl in both phases. All the activities are calculated from one Gibbs energy function (Eq. C1), which in an energy-composition diagram (Fig. 28) graphically corresponds to a common tangent line at two

points of the function. Consequently, the Gibbs energy function must contain at least two inflexion points.

$$\Delta G^{mixing} = RT \cdot \sum_i x_i \cdot \ln(a_i) \quad (C1)$$

The vertical axis intercepts of the tangent line define the equal chemical potentials of NaCl and KCl, at $x(KCl)=0$ and at $x(KCl)=1$, respectively (Fig. 28). By selecting a certain standard excess Gibbs energy function with only two variables (see Eq. 19 and Table 9), these intercepts can be used to calculate those two variables. The temperature and pressure dependence of these variables can be estimated from a set of experimental data of coexisting solid phases at a variety of temperatures and pressures. The resulting Gibbs energy function at 400°C (according to Eq. C1) that is illustrated in Fig. 28 contains two inflexion points between a solid phase with composition a in equilibrium with a solid phase with composition b . The function displays a single minimum without any inflexion points at 700°C, at temperatures above the maximum value of the solvus, i.e. 495°C.

Appendix D

Determination of activity coefficients of a coexisting liquid and solid phase

The definition of the excess Gibbs energy for solid solutions (Eqs. 19b and 21) is used to determine the activity coefficients of NaCl and KCl in the liquid solution at thermodynamic equilibrium (Eqs. 13 to 15). The excess Gibbs energy of both liquid and solid solution above 495°C contain a single minimum in NaCl-KCl solutions, without inflexion points (Fig. 28). In Fig. 29, a liquid solution with the composition a' is in equilibrium with a solid phase of composition a . The tangent lines at point a on the solidus and at point a' on the liquidus intersect the vertical axis at $x(KCl)=0.0$. The difference between these intersections is defined by the melting of pure NaCl (ΔG_{NaCl}^0), see also Appendix B. The intersections with $x(KCl)=1.0$ is defined by the melting of pure KCl (ΔG_{KCl}^0). Unknown activity coefficients of NaCl and KCl in the liquid solution can be directly obtained from a selected general excess Gibbs energy function, such as a fourth-suffix Margules equation, the definitions of Gibbs energy of the solid solution and the melting behaviour of the pure endmembers. Figure 29 illustrates at 700°C the possibility of the coexistence of two pairs of liquid–solid phases in equilibrium: 1. in NaCl-rich solutions (points a and a'), and 2. in KCl-rich solutions (points b and b').

References

Anderko A, Pitzer KS (1993) Phase equilibria and volumetric properties of the system KCl-H₂O and NaCl-KCl-H₂O above 573 K:

- Equation of state representation. *Geochim Cosmochim Acta* 57:4885–4897
- Anderson G (2008) *Thermodynamics of natural systems*. Cambridge University Press, Cambridge
- Bakhuis-Roozeboom HW (1899) Erstarrungspunkte der Mischkristalle zweier Stoffe. *Z Phys Chem* 30:289–327
- Bakker RJ (2003) Package *FLUIDS* 1. Computer programs for analysis of fluid inclusion data and for modelling bulk fluid properties. *Chem Geol* 194:3–23
- Bakker RJ (2012) Can the vapour phase be neglected to estimate bulk salinity of halite bearing aqueous fluid inclusions? *Cent Eur J Geosci*. doi:10.2478/s13533-011-0046-y
- Barrett WT, Wallace WE (1954) Studies of NaCl-KCl solid solutions. I: heats of formation, lattice spacings, densities, Shottky defects, and mutual solubilities. *J Am Chem Soc* 76:366–369
- Becker SP, Fall A, Bodnar RJ (2008) Synthetic fluid inclusions. XVII. PVTX properties of high salinity H₂O-NaCl solutions (>30 wt% NaCl): application to fluid inclusions that homogenize by halite disappearance from porphyry copper and other hydrothermal ore deposits. *Econ Geol* 103:539–554
- Bhardwaj MC, Roy R (1971) Effect of high pressure on crystalline solubility in the system NaCl-KCl. *Phys Chem Solids* 32:1603–1607
- Bodnar RJ (1992) The system H₂O-NaCl (abstract). PACROFI IV, Program and Abstracts, University of California, Riverside, 108–111
- Bodnar RJ (1993) Revised equation and table for determining the freezing point depression of H₂O-NaCl solutions. *Geochim Cosmochim Acta* 57:683–684
- Bodnar RJ (1994) Synthetic fluid inclusions: XII. The system H₂O-NaCl. Experimental determination of the halite *liquidus* and isochores for a 40 wt% NaCl solution. *Geochim Cosmochim Acta* 58:1053–1063
- Bodnar RJ, Sterner SM, Hall DL (1989) SALTY: a FORTRAN program to calculate compositions of fluid inclusions in the system NaCl-KCl-H₂O. *Comput Geosci* 15:19–41
- Bukhalova GA, Bergman AG (1955) Quaternary reciprocal systems of the fluorides and chlorites of sodium, potassium, calcium, and barium as the basis for fluxes for the remelting of secondary light metals. *Zh Priklad Khim* 28:1266–1274
- Bunk AJH, Tichelaar GW (1953) Investigations in the systems NaCl-KCl. *Kon Ned Akad Wetensch Proc B* 56:375–384
- Campbell AR, Lundberg SAW, Dunbar NW (2001) Solid inclusions of halite in quartz: evidence for the halite trend. *Chem Geol* 173:179–191
- Chanh NB (1964) Equilibres des systems binaires d'halogenures de sodium et potassium a l'etat solide. *J Chim Phys* 61:1428–1433
- Chase MW, Davies CA, Downey JR, Frurip DJ, McDonald RA, Syverud AN (1985) *JANAF Thermochemical Tables*, 3rd Ed. *J Phys Chem Ref Data* 14(1)
- Chou I-M (1982) Phase relations in the system NaCl-KCl-H₂O. Part I: differential thermal analysis of the NaCl-KCl *liquidus* at 1 atmosphere and 500, 1000, 1500, and 2000 bars. *Geochim Cosmochim Acta* 46:1957–1962
- Chou I-M (1987) Phase relations in the system NaCl-KCl-H₂O. III: solubilities of halite in vapor-saturated liquids above 445°C and redetermination of phase equilibrium properties in the system NaCl-H₂O to 1000°C and 1500 bars. *Geochim Cosmochim Acta* 51:1965–1975
- Chou I-M, Sterner SM, Pitzer KS (1992) Phase relations in the system NaCl-KCl-H₂O: IV. Differential thermal analysis of the *liquidus* in the KCl-H₂O binary, the *liquidus* in the NaCl-KCl-H₂O ternary, and the *solidus* in the NaCl-KCl binary to 2 kb pressure, and a summary of experimental data for thermodynamic-PTX analysis of solid-liquid equilibria at elevated P-T conditions. *Geochim Cosmochim Acta* 56:2281–2293
- Driesner T, Heinrich CA (2007) The system H₂O-NaCl. Part I. Correlation formulae for phase relations in the temperature-pressure-composition space from 0 to 1000°C, 0 to 5000 bar, and 0 to 1 *X*_{NaCl}. *Geochim Cosmochim Acta* 71:4880–4901
- Green EJ (1970) Predictive thermodynamic models for mineral systems. I. Quasi-chemical analysis of the halite-sylvite subsolidus. *Am Min* 55:1692–1713
- Goldstein RH, Reynolds TJ (1994) Systematics of fluid inclusions in diagenetic minerals. SEPM Short Course 31, Society for Sedimentary Geology, US of A
- Gunter WD, Chou I-M, Girsperger S (1983) Phase relations in the NaCl-KCl-H₂O II: differential thermal analysis of the halite *liquidus* in the NaCl-H₂O binary above 450°C. *Geochim Cosmochim Acta* 47:863–873
- Hall DL, Sterner SM, Bodnar RJ (1988) Freezing point depression of NaCl-KCl-H₂O solutions. *Econ Geol* 83:197–202
- Heide K, Brückner U (1967) Grundlagen zur Phasenanalyse von Salzgesteinen. 1. Die binären Teilsysteme des anhydritischen Hartsalzes KCl-NaCl und KCl-CaSO₄. *Chem Erde* 26:235–255
- Kamenetsky VS, Sharygin VV, Kamenetsky MB, Golovin AV (2006) Chloride-carbonate nodules in kimberlites from the Udachnaya Pipe: alternative approach to the evolution of Kimberlite Magmas. *Geochem Intern* 44:935–940
- Keevil NB (1942) Vapor pressures of aqueous solutions at high temperatures. *J Am Chem Soc* 64:841–850
- Linke WF (1965) Solubilities: inorganic and metal-organic compounds, vol 2. American Chemical Society, Washington
- Lumsden J (1952) *Thermodynamics of alloys*. Institute of metals. Addison-Wesley Press, London
- Luova P, Muurien M (1967) Thermodynamic studies on the systems NaCl-KCl and KBr-KI. *Ann Univ Turk, Series A* 110:1–15
- Nacken R (1918) Über die Grenzen der Mischkristallbildung zwischen Kaliumchlorid und Natriumchlorid. *Sitzungsber Preuss Akad Wiss Phys Math Kl* 192–200
- Oonk HAJ (1981) Phase theory—the thermodynamics of heterogeneous equilibria. *Studies in modern thermodynamics*, vol. 3. Elsevier, Amsterdam, 269
- Pelton AD, Gabriel A, Sangster J (1985) *Liquidus measurements and coupled thermodynamic-phase-diagram analysis of the NaCl-KCl system*. *J Chem Soc Faraday Trans* 81:1167–1172
- Potter RW II, Clyne MA, Brown DL (1978) Freezing point depression of aqueous sodium chloride solutions. *Econ Geol* 73:284–285
- Prausnitz JM, Lichtenthaler RN, de Azevedo EG (1986) *Molecular thermodynamics of fluid-phase equilibria*. Prentice-Hall, Englewood Cliffs, NJ 07632, 600
- Ravich MI, Borovaya FE (1949) Phase equilibria in ternary water-salt systems at high temperatures. *Akad Nauk SSSR, Izv Sekt Fiziko-Khimi Anal* 19:69–81
- Ravich MI, Borovaya FE (1950) Crystallization of melts of chlorides of K and Na in the presence of water vapor (in Russian). *Izvest Sektora Fiz-Khim Anal Inst Obshch i Neorg Khim, Akad Nauk SSSR* 20:165–183
- Robie RA, Hemingway BS, Fisher JR (1979) Thermodynamical properties of minerals and related substances at 298.15 K and 1 bar (105 Pascals) pressure and higher temperatures. *USGS Bull* 1452:1–455
- Rubleva VV, Bergman AG (1956) Equilibrium diagram of the Na₂Cl₂-K₂Cl₂-CaSO₄ system. *Zhurnal Obshchei Khimi* 26:651–655
- Sabouraud C (1994) Solid and fluid inclusions of evaporites; gypsum. *Evaporite sequences in petroleum exploration*; 1, *Geol Methods*, 136–145
- Sourirajan S, Kennedy GC (1962) The system H₂O-NaCl at elevated temperatures and pressures. *Am J Sci* 260:115–141
- Sterner SM, Hall DL, Bodnar RJ (1988) Synthetic fluid inclusions. V. Solubility relations in the system NaCl-KCl-H₂O under vapor-saturated conditions. *Geochim Cosmochim Acta* 52:989–1005

- Sterner SM, Chou I-M, Downs RT, Pitzer KS (1992) Phase relations in the system NaCl-KCl-H₂O: V. Thermodynamic-PTX analysis of solid-liquid equilibria at high temperatures and pressures. *Geochim Cosmochim Acta* 56:2295–2309
- Taylor JLR (1995) Guide for the use of the international system of units (SI). NIST Special Publication 811, US Government Printing Office, Washington
- Thompson JB, Waldbaum DR (1969) Analysis of the two-phase region halite-sylvite in the system NaCl-KCl. *Geochim Cosmochim Acta* 33:671–690
- van Laar JJ (1910) Über Dampfspannungen von binären Gemischen. *Z Phys Chem* 72:723–751
- Vesnin YI, Zakovryashin SP (1979) About the decay of solid solutions KCl-NaCl. *Solid State Comm* 31:635–640
- Waldbaum DR (1969) Thermodynamic mixing properties of NaCl-KCl liquids. *Geochim Cosmochim Acta* 33:1415–1427
- Wilkinson JJ (2003) On diagenesis, dolomitisation and mineralisation in the Irish Zn-Pb orefield. *Mineral Deposita* 38:968–983
- Wohl K (1946) Thermodynamic evaluation of binary and ternary liquid systems. *Trans Am Ing Chem Eng* 42:215–249